EFFECT OF LAND USE AND GROUNDWATER FLOW PATH ON SUBMARINE GROUNDWATER DISCHARGE NUTRIENT FLUX

THESIS SUBMITTED TO THE GRADUATE DIVISION OF THE UNIVERSITY OF HAWAI'I AT MĀNOA IN PARTIAL FULFILLMENT OF THE REQUIREMENTS FOR THE DEGREE OF

MASTER OF SCIENCE

IN

GEOLOGY AND GEOPHYSICS

JULY 2015

By

James M. Bishop

Thesis Committee:

Craig R. Glenn
Henrieta Dulaiova
Brian N. Popp

Acknowledgments

I thank my advisor, Craig Glenn, for helping with my thesis project from conception to completion. I also thank Henrieta Dulaiova for help in the field and in the office. Daniel Amato helped tremendously in the field and with the data. I would like to thank Brian Popp, Aly El-Kadi, Robert Whittier, Celia Smith, and Joe Fackrell for enlightening discussions and critiques of this work and for reviewing an earlier draft of the thesis. I also thank Russell Sparks from the Maui Division of Aquatic Resources, Joe Mendonca from the Maui Department of Water Supply, Napua Barrows from the Waiehee Limu Restoration Project, and Maui Land and Pineapple Company, Inc., for logistic support. Finally, we thank Joe Fackrell, Chris Shuler, Sam Wall, and Jeff Strotzki for their help with our fieldwork. We thank the Geological Society of America for a Graduate Student Research Grant. This research was funded in part by a grant/cooperative agreement from the National Oceanic and Atmospheric Administration, Project R/HE-17, which is sponsored by the University of Hawai'i Sea Grant College Program, SOEST, under Institutional Grant No. NA09OAR4170060 from NOAA Office of Sea Grant, Department of Commerce. The views expressed herein are those of the authors and do not necessarily reflect the views of NOAA or any of its subagencies. UNIHI-SEAGRANT-JC-13-32.

Abstract

Fertilized agricultural lands, wastewater injection, and areas with high septic system and cesspool density each have potential to contribute excess nutrients to coastal waters of Maui via submarine groundwater discharge (SGD). We investigated the connection between such land uses and coastal waters and quantified their respective impacts around the island of Maui, Hawai'i using a numerical groundwater model, O isotopic composition of H_2O, and N and O isotopic compositions of dissolved nitrate to identify the groundwater pathways, recharge elevations, and nitrate sources. Fresh and total SGD rates and nutrient fluxes were quantified using ^{222}Rn mass balance modeling.

Low nitrate + nitrite (N+N) SGD fluxes (24 moles/d) were measured where groundwater flowed beneath primarily undeveloped land on transit to the coast. By contrast, sugarcane and pineapple fields discharge the largest amount of N to coastal waters via SGD of any land use type (4900 moles/d), and despite the much smaller freshwater SGD flux these rates are substantially larger than N fluxes from the State's largest rivers (avg. 700 moles/d). Septic systems, cesspools, and near coast wastewater injection wells also contribute N+N to groundwater and coastal waters, though in much smaller quantities. This study demonstrates that numerical groundwater modeling combined with geochemical modeling can be used to determine sources and flux of nutrients in SGD and provides a unique, original, and practical framework for studying the effect of land use and its impact on nutrient delivery to coastal waters.

Table of Contents

Effect of Land Use and Groundwater Flow Path on Submarine Groundwater Discharge Nutrient Flux

James M. Bishop[1], Craig R. Glenn[1], Daniel W. Amato[2], Henrieta Dulaiova[1]
[1]Department of Geology and Geophysics, University of Hawai'i at Manoa
[2]Department of Botany, University of Hawai'i at Manoa

1. Introduction

Fertilized agricultural lands, wastewater injection, and areas with high septic system density each have potential for contributing excess nutrients to coastal waters of islands via submarine groundwater discharge (SGD). It has been hypothesized for the island of Maui that excess nutrient loading via SGD is a causal factor fueling the macroalgae blooms that have been smothering corals and economically and aesthetically fouling beaches since the late 1980's (e.g. Soicher and Peterson, 1997; Dollar and Andrews, 1997; Laws et al., 2004; Cesar and van Beukering, 2004; van Beukering and Cesar, 2004; Street et al., 2008; Dailer et al., 2010; Dailer et al., 2012). A first step in limiting nutrient additions to coastal waters is to identify the source of nutrients. While methodologies for source tracking of nutrients to receiving waters from overland flow are well established (Borah and Bera, 2004), methods for determining nutrient sources in SGD are less well developed. The purpose of this study is to identify the sources of nutrients delivered to coastal waters via SGD.

Relatively few studies have focused specifically on trying to identify the terrestrial source of nutrients in SGD. One such study on Long Island, New York found that high-density development was correlated with high nitrate discharge rates via SGD (Young et al., 2015). Another study on Kauai, Hawaii found correlations between the amount of proximal agricultural land and N+N concentrations, which suggested fertilizers as the primary N+N source (Knee et al., 2008). On Hawai'i Island, similar correlations were found between N+N concentrations and proximity of golf courses, again implying a fertilizers source (Knee et al., 2010). Such studies have strongly suggested a link between land use and specific SGD nutrient concentrations, but they have relied solely on correlations with proximal land use, and have not

considered groundwater flowpaths and thus not the full variety of possible land use nutrient additions to groundwater as they transit to the coast.

In this paper we combine numerical groundwater modeling, geochemical mass balance modeling, and stable isotope biogeochemistry to identify specific land use practices on Maui that contribute nutrients to coastal waters via SGD and quantify the amount of nutrients delivered from those sources. We utilize a numerical groundwater model (Whittier et al., 2010) to identify the specific groundwater flow pathways to the coast, $\delta^{18}O$ of H_2O to determine groundwater recharge elevations, $\delta^{15}N$ and $\delta^{18}O$ of dissolved nitrate to determine nitrate sources, and ^{222}Rn mass balance modeling to quantify fresh and total SGD rates. With these tools we (1) quantify the flux of nutrients to coastal waters via SGD in different areas of Maui, (2) identify specific land use practices that contribute nutrients to the coastal zone via SGD, and (3) calculate the flux of nutrients delivered to specific coastal zones from different land use practices. Our study demonstrates that numerical groundwater modeling combined with geochemical modeling is a robust method for determining the sources and flux of nutrients in SGD. The results presented here also illustrate how such work can provide site specific information of value to local land use managers and planners regarding the magnitude of nutrients contributed to coastal waters from different land use practices.

2. Regional and Hydrogeologic Setting

The island of Maui (Fig. 1) is the second largest island in the Hawaiian Island chain. It is comprised of two separate basaltic shield volcanoes that overlap to form an isthmus between them (Stearns and Macdonald, 1942). The West Maui volcano has a maximum elevation of 1764 meters and Haleakala, the volcano comprising East Maui, has an elevation of 3055 meters. Rainfall in Hawai'i is driven primarily by a combination of trade winds and orographic effect. Trade winds are persistent and blow from the northeast resulting in the north and eastern facing (windward) slopes generally receiving higher amounts of rainfall than south and west facing (leeward) slopes. Rainfall patterns in Hawai'i are extremely diverse

and rainfall gradients can be exceptionally steep (see Giambelluca et al., 2011). On Maui, northeast facing, higher elevation areas can receive rainfall upwards of 1000 cm per year, while the leeward Kihei region in southern Maui, one of the driest areas in the State, receives only 38 cm per year of rainfall on average (Giambelluca et al., 2013).

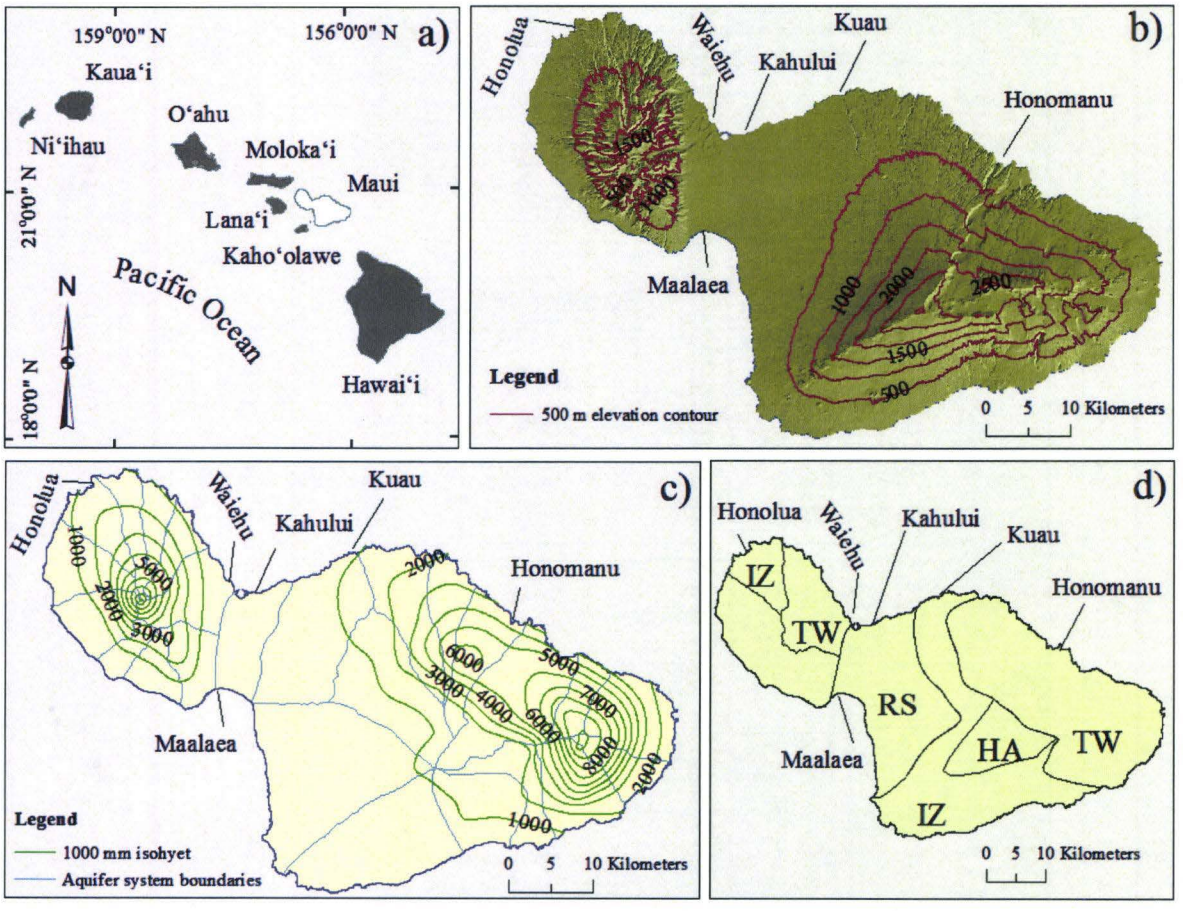

Fig.1 (A) Hawaiian Islands with Maui shown in white. (B) Shaded relief map of Maui Island showing 500 m elevation contours. (C) Maui aquifer sectors in light blue and 1000 mm rainfall isohyets in green. (D) Local meteoric water line climate zones, adopted and modified from Scholl et al. (2002), used in recharge elevation calculations. Coastal areas investigated during this study are indicated. Rainfall data from Giambelluca et al. (2013); DEM from NOAA (2007); aquifer sectors from State of Hawai'i (2008).

A conceptual hydrogeologic model for the island of Maui is shown in Fig. 2. The island was built primarily by interbedded basaltic lavas. Near vertical dikes of low permeability basalt radiate outward from the calderas of each volcano and have cut through the bedded lavas. Along the coast and in the isthmus between the two volcanoes sedimentary deposits locally termed caprock impede the discharge of fresh groundwater at the coast (Engott and Vana, 2007). Fresh groundwater on Maui occurs primarily as either a basal freshwater system or high level, dike-impounded water. The basal freshwater system consists of a lens-shaped body of freshwater floating above more dense saline water that intrudes from the coast. Water levels in the basal system slope gently upward from the coast at rate of about 0.3 m/km near Kahului (Burnham et al., 1977), though gradients can be much steeper in areas with substantial caprock. Unlike the basal system, dike impounded water can have hydraulic head thousands of feet above sea level due to the low permeability of dike rock (Engott and Vana, 2007), although the lateral extent of the dike impounded water is relatively small.

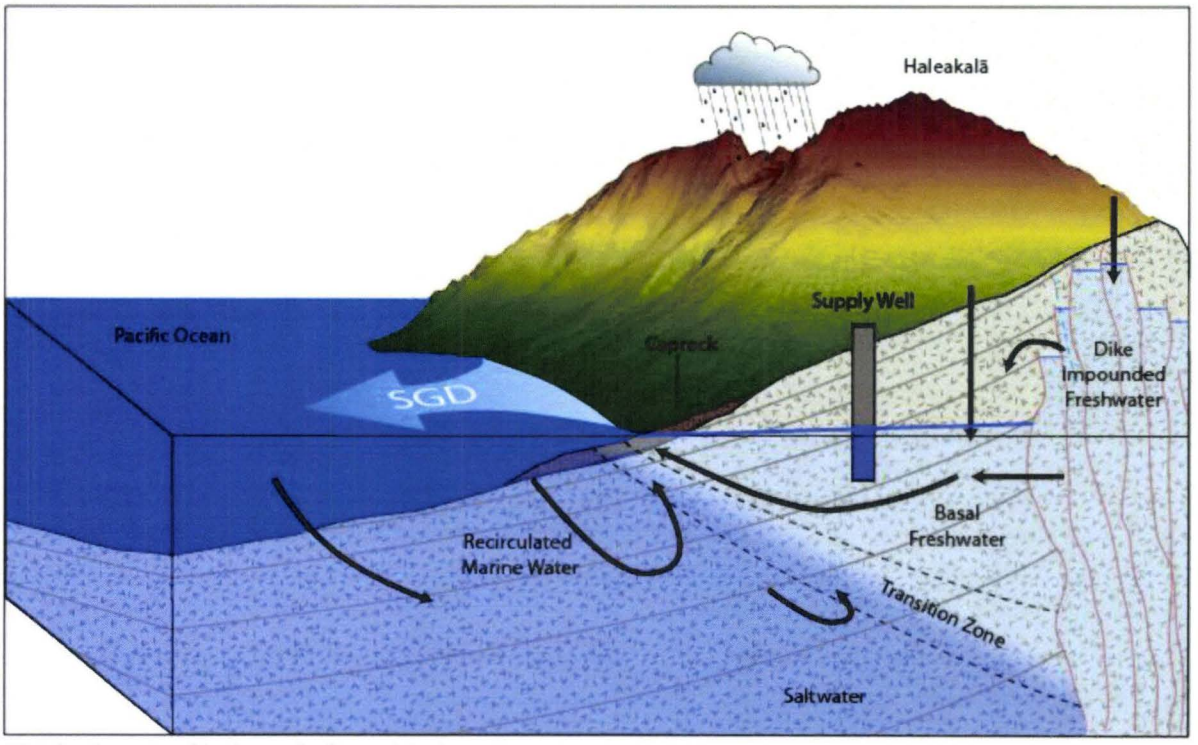

Fig. 2. Conceptual hydrogeologic model of Maui.

3. Methods

3.1 Land Use and Study Sites

At low and moderate elevations forests dominate the landscape of wetter regions of Maui, while grasses, shrubs, and development cover drier areas. High elevations are dry and comprised of shrubs and grasslands. Central Maui is currently covered by approximately 160 km^2 of commercial sugarcane and had 45 km^2 of pineapple produced in the 1980's, though pineapple cultivation has since been reduced to only 7 km^2 in 2015. On west Maui, pineapple and sugarcane were produced for most of the 20^{th} century but sugarcane production ceased in 1999 and pineapple has been uncultivated since 2006.

To evaluate the effects of land use on nutrient concentrations to groundwater and coastal waters we chose coastal field areas that occurred downslope of specific dominant types of land use (Fig. 3; Table 1). Land use categories were based on a 2005 NOAA land cover map (NOAA, 2012) for Maui that delineated 25 land use types. Different land use types were reclassified to 3 groups: agricultural land, developed land, and undeveloped land. An agricultural land use map from the State of Hawai'i Office of Planning, drafted between 1978-1980, was used to determine the different types of agriculture. We used this map because groundwater flow in Hawaiian aquifers occurs on multi-decadal scales (Kelly et al., 2015) and hence chemical legacy effects of previous agricultural practices may still be present in the aquifers. The agricultural land use map was used to subdivide NOAA land cover agricultural polygons into 5 agricultural land use sub-categories: sugarcane, pineapple, macadamia orchards, agriculture unspecified, and commercial dairies.

We also consider and overlay cesspools and septic tanks, collectively called on-site disposal systems (OSDS). OSDS risk to groundwater and coastal waters for different areas on Maui was estimated and ranked by Whittier and El-Kadi (2014) and is utilized in this study to identify areas to investigate for OSDS contamination. Areas were designated either high or low OSDS density. High OSDS density were regions where OSDS exceeded 40 units/mi^2, which is the density at which OSDS begin contaminating

groundwater quality, as determined by the USEPA (Yates, 1985). Wastewater injection wells were identified from the State of Hawai'i's Commission on Water Resources Management well index database and were also integrated in our analysis. The County of Maui Wastewater Reclamation Division provided injectate volume and total nitrogen and phosphorus concentrations for the Kahului Wastewater Reclamation Facility.

Table 1. Field areas investigated in this study. The land uses that were assumed to contribute nutrients to groundwater and coastal water are listed.

Field Area	Potential Land Use Sources of Nutrients
Kuau	Sugarcane, pineapple, moderate OSDS risk
Maalaea	sugarcane, low-vol. wastewater injection
Kahului	sugarcane, high-vol. wastewater injection, moderate OSDS risk
Honolua	Pineapple
Waiehu	high OSDS risk, agriculture
Honomanu	Undeveloped land

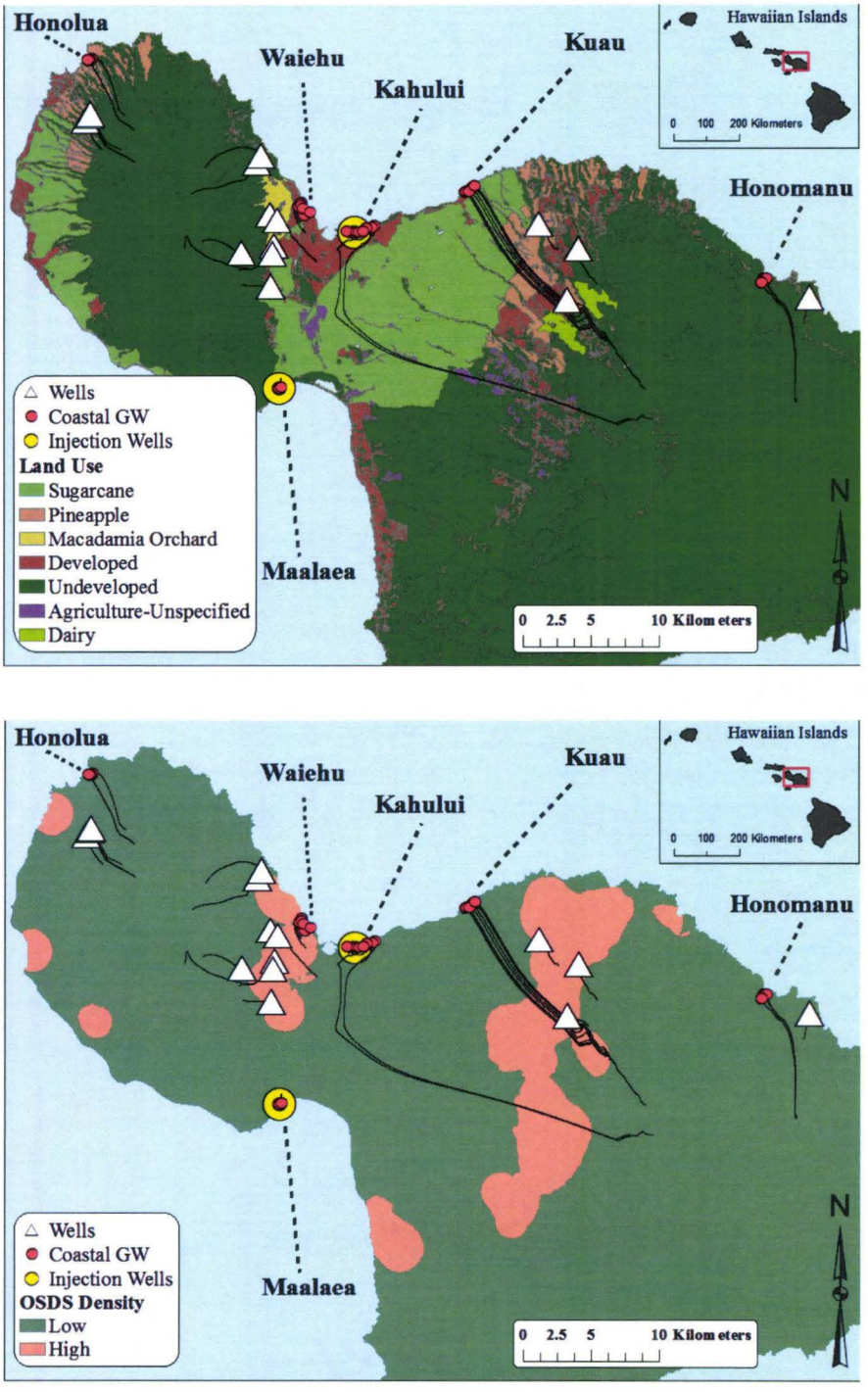

Fig. 3. Map of field sites. Land use (top) and OSDS density (bottom) are shown. Black lines indicate MODPATH derived groundwater flow paths (discussed below). Red circles indicate coastal groundwater sampling locations, white triangles are fresh groundwater supply well samples, and yellow dots show wastewater injection well locations utilized in this study.

3.2 Water Sampling and Analysis

Fieldwork was conducted during July 2012, July 2013, and March and April 2014. Water samples were collected from public water supply wells, coastal springs, beachface piezometers, and coastal surface waters. All samples were analyzed for the dissolved inorganic nutrients: silica (Si), nitrate and nitrite (N + N), ammonium (NH_4^+), and phosphate (PO_4^{3-}), using a Seal Analytical AA3Nutrient Autoanalyzer at the University of Hawai'i SOEST Laboratory for Analytical Biogeochemistry (S-Lab). Over the course of the 3 sampling periods 30 nutrient samples were collected in duplicate and the uncertainty associated with duplicate analysis was calculated using relative percent difference (RPD; the absolute value of the difference as a percentage of the mean of the two samples). Average RPD was 4% for Si, 15% for N+N, 14% for PO_4^{3-}, and 62% for NH_4^+. $\delta^{18}O$ in water (H_2O) was analyzed using a Picarro Cavity Ringdown Mass Spectrometer. Oxygen isotopic compositions were normalized to internal lab reference waters and are expressed in δ-notation in per mil (‰) relative to VSMOW. Samples with adequate nitrate concentration (≥1 μM) were analyzed for the nitrogen and oxygen isotopic composition of dissolved nitrate using the denitrifier method (Sigman et al., 2001, Casciotti et al., 2002, McIlvin and Casciotti, 2011). For samples that had a nitrite concentration greater than 1% of the nitrate concentration, nitrite was removed using sulfamic acid during sample preparation (Granger et al., 2006), prior to N and O isotopic analysis. Samples were analyzed on a Thermo-Finnigan MAT252 mass spectrometer interfaced to a Thermo Finnigan Gasbench II with the Thermo Scientific Denitrification Kit. Analyses of N and O isotopic compositions of dissolved nitrate were normalized with nitrate-N and nitrate-O reference materials USGS-32, USGS-34, and USGS-35 relative to AIR and are expressed in δ-notation in per mil (‰) relative to AIR and VSMOW, respectively. The error associated with duplicate analysis (n = 18) of stable isotopes, using the standard error of the estimate, was 0.05 ‰ for $\delta^{18}O_{H2O}$, 0.48‰ for $\delta^{18}O_{NO3}$, and 0.73‰ for $\delta^{15}N_{NO3}$. In situ temperature, salinity, conductivity, pH, and dissolved oxygen concentration were collected with multiparameter sondes (YSI 6600 V2-4, YSI EXO2) at the time of sample collection.

3.3 Coastal Groundwater Endmembers and Salinity Unmixing

In order to compare nutrient concentrations among field areas and to assign a nutrient value to use in SGD nutrient flux calculations (described below) we determined coastal groundwater endmember nutrient concentrations representative of an entire field area. To do this, we normalize brackish coastal groundwater concentrations to find the fresh groundwater concentration by fitting a linear regression to nutrient concentration versus salinity. Then, using the regression equation, we calculate the nutrient concentration that was equal to fresh groundwater salinity. The fresh groundwater salinity used to calculate nutrient endmember was the salinity of the most proximal public supply well sampled.

In order to compare the nutrient concentrations and $\delta^{18}O_{H2O}$ values among individual samples that were collected with varying amounts of seawater dilution, samples were all 'unmixed' (normalized) to the fresh groundwater endmember as (Hunt and Rosa, 2009):

$$C_1 = C_{mix} + (C_{mix} + C_2) \times (S_{mix} + S_1)/(S_2 - S_{mix}) \qquad (1)$$

where C_1 is the expected concentration or δ value of the sample prior to seawater dilution, C_{mix} is the concentration or δ value of the sample to be unmixed, C_2 is the concentration or δ value of the seawater endmember, S_{mix} is the salinity of the sample to be unmixed, S_1 is the salinity of the fresh groundwater endmember, and S_2 is the salinity of the marine endmember. Equation 1 removes nutrient concentration dilution and ^{18}O enrichment that results from freshwater mixing with seawater so that all results can be directly compared on a freshwater-only basis. Unmixed concentrations for samples from a particular field area were calculated using endmembers specific to that area. The marine salinity and concentration used in Equation 1 were from the highest salinity coastal water sample from a particular area. The fresh groundwater salinity was chosen from the well most proximal to each field area, or for the case at Maalaea which had no proximal wells, the mean of all wells sampled on the island. Salinities in wells ranged from 0.05 to 0.40.

3.5 Groundwater Flowpaths

Groundwater flowpaths were determined using a combination of MODFLOW modeled groundwater heads (Whittier et al., 2010), MODPATH, the oxygen isotopic composition of water, groundwater recharge data, and local meteoric water lines for different climate zones (Scholl, 2002). MODFLOW (Harbaugh, 2005) is a three dimensional finite difference groundwater model used to calculate steady state and transient groundwater flow. MODPATH (Pollock, 2012) is a model that computes three dimensional groundwater flowpaths, called particle paths, using the output from MODFLOW modeled groundwater heads. Using MODPATH, we created imaginary particles at each sampling location and tracked those particles from the sampling location to their origin. For wells, particle paths were created at the bottom of the screened interval of the well. Coastal groundwater particle paths were created at the bottom of the four layer model (Whittier et al., 2010) in order to generate particle paths that best reflected actual flowpaths in the basal lens. The origin of each path was subsequently modified after calculating the recharge elevation using the methods of Scholl et al. (1996) and described below.

Recharge elevations, and thus particle path origins, were determined using a groundwater recharge rate raster file (10m x 10m resolution; Whittier and El-Kadi, 2014), the $\delta^{18}O_{H20}$ in coastal groundwater samples, and the local meteoric water lines of Scholl et al. (2002). Because aquifers on Maui are mostly unconfined (Gingerich, 2008) except for carbonate caprock that occurs near the coast (Stearns and Macdonald, 1942), the isotopic composition of fresh coastal groundwater can be assumed to represent the integration of isotopic compositions in precipitation that fell along the entire groundwater flowpath (Scholl et al., 1996). We assume there is no net isotopic fractionation between the precipitation and recharge. The isotopic composition of fresh coastal groundwater is the recharge-weighted average of the isotopic composition of precipitation from the recharge elevation to the coast. Recharge elevation is determined by finding the elevation at which measured groundwater isotopic composition matches the calculated, recharge-weighted, isotopic composition following the equation of Scholl et al. (1996):

$$\delta^{18}O_{sample} = \frac{\sum_{elev=1}^{n}(\delta^{18}O)_n(R)n}{\sum_{elev=1}^{n}(R)_n} \quad (2)$$

where $(\delta^{18}O)_n$ is the isotopic value of precipitation calculated for raster cell *n*, $(R)_n$ is the recharge rate of raster cell *n*, and $\delta^{18}O_{sample}$ is the measured $\delta^{18}O$ value in the groundwater sample. A raster dataset of the isotopic composition of precipitation was created by multiplying the elevation in each cell of a 10 m vertical resolution digital elevation model (NOAA, 2007) by the $\delta^{18}O$ in precipitation vs. elevation regression equations for the different climate zones from Scholl et al. (2002). Particle paths are shown in Fig. 3. An important caveat is that that MODPATH does not take in to account dispersion, which may be an important component in determining particle path trajectories if there is a high dissolved load. As such, the particle paths presented are idealized paths.

The elevation versus isotopic composition of precipitation relationships developed by Scholl et al (2002) were defined for different climates zones on Maui and include the tradewind zone (TW), rain shadow zone (RS), and high altitude zone (HA) (Fig. 1). TW encompassed samples from Honomanu and RS encompassed samples from Kahului and Maalaea. To better characterize samples from Kuau, which were located in the transition between TW and RS zones, we created a third climate zone called the intermediate zone (IZ). IZ has a slope and intercept that was the mean of the slopes and intercepts from the TW and RS zones and was nearly parallel to the isotopic composition versus slope regressions those two zones. Similar elevation-versus-precipitation relationships have not been developed for West Maui and as such there is no pre-defined climate zone to apply to the Waiehu and Honolua field areas. We assigned the elevation versus precipitation relationship that was most suitable for Waiehu and Honolua based on our knowledge of rainfall, trade winds, and measured groundwater isotopic compositions.

3.6 Statistical Analysis

We conducted a multiple regression analysis to identify a linear relationship between the salinity unmixed nutrient concentration measured at all sampling locations (dependent variable) and the length of different land use types overlying all groundwater flow paths (independent variables). To test for significance and

F-test was used at the 95% confidence level. Key assumptions of multiple linear regression relevant to this analysis include linearity between independent and dependant variables, normality of residuals, and homoscedasticity (Keith, 2006). All assumptions were examined and are presented with the results.

3.7 Submarine Groundwater Discharge Rates and Nutrient Fluxes

In order to quantify submarine groundwater discharge rates at each field area we used stationary radon time series to conduct a non-steady-state mass-balance model (Burnett and Dulaiova, 2003). We coupled the time series calculated rates with radon coastal surface water surveys (Dulaiova et al., 2010) to scale the stationary time series calculated fluxes by the mean fluxes measured along the coastline transected by the coastal survey, as detailed below. Radon in surface waters was measured using a Rn-in-air monitor (RAD-Aqua, Durridge Inc., Billerica MA, USA) connected to an air-water exchanger that received water from a peristaltic pump (time series) or a bilge pump (surveys). Conductivity, temperature, and depth (CTD) were monitored at the pump hose inlet (time series and survey) and on the seafloor bottom (time series). Wind speed and air temperature were collected from either Kahului (WBAN 22516) or Kapalua (WBAN 22552) airport weather stations. We used an offshore ^{222}Rn activity of 64 dpm/m^3, which was derived from its parent ^{226}Ra activity identified by Street et al. (2008) and a ^{226}Ra supported ^{222}Rn activity of 79 dpm/m^3, as measured by Street et al. (2008) at station MA3 on Maui. Groundwater residence times were assumed to be 12.42 hours, the length of a tidal cycle. We used an atmospheric radon activity of 30 dpm/m^3 (Kelly, 2012). Discrete coastal groundwater were analyzed within 12 hours of collection using a RAD-H_2O system (Durridge), then time-corrected for decay.

3.7.1 Stationary Time Series Measurements

All time series were conducted during March and April 2014, except for Kuau which was conducted July 2013. Radon measurements were integrated over 30 minute periods. A salinity depth profile was collected at the time series location in order to characterize the thickness of the mixed-salinity brackish SGD plume, which disperses from land and floats on top of marine water. In order to account for changes in the thickness of the brackish SGD plume over a tidal cycle, we subtracted the marine layer thickness

measured during the depth profile from the total depth of the water column measured by the CTD. We then scaled the ^{222}Rn inventories to the depth of the mixed-salinity SGD layer at the corresponding cycle.

3.7.2 Radon Surface Water Surveys

Surface water surveys were conducted during July 2013 with the exception Maalaea and Honolua, which were conducted in March 2014 and August 2012, respectively. Radon surveys were conducted by motoring a boat parallel to shore at approximately 5 km/hr while the bilge pump was constantly supplying surface water to the air-water exchanger. Radon measurements were integrated over 5 minute periods. SGD fluxes were calculated using ^{222}Rn box model of Dulaiova et al. (2010). The coastal boxes used were determined as the perpendicular distance from the shore to each radon data point, and the half distance from one data point to the other along the shore. The depth of the coastal box was the thickness of the mixed salinity layer determined by salinity depth profiles, which were taken periodically.

3.7.3 SGD Flux Scaling

While survey-calculated fluxes have been used as standalone measurements of discharge rates (Burnett and Dulaiova, 2003; Dulaiova et al., 2005; Dulaiova et al., 2010), these only represent a snapshot of SGD rates and not a tidal average. We therefore used the survey calculated fluxes in a relative sense to scale the time series calculated flux. This thus combines the spatial resolution of the survey fluxes with the temporal resolution of the time series flux. The primary reason for using scaled SGD rates is that, for the purpose of understanding the effect of land use on coastal nutrient concentrations via SGD, it is more beneficial to calculate fluxes for the entire length of coastline affected by a particular type of land use, not just a single spring. A tacit assumption in the scaling is that the ratio of fresh groundwater to recirculated seawater in SGD remains constant over the survey area.

3.7.4 Calculating Fresh SGD Flux and Nutrient Flux

The methods described above are used to calculate the total (fresh + saline) SGD fluxes. Land derived nutrients in SGD are contained primarily in the fresh portion of SGD. Therefore, in order to obtain a

meaningful nutrient flux, we calculate the freshwater fraction of total SGD in order to obtain a freshwater SGD flux. Furthermore, this approach allows for direct comparison of the fresh SGD nutrient flux to the freshwater nutrient flux from rivers in Hawaii. The fresh SGD nutrient flux is then simply the product of the fresh SGD rate and the groundwater endmember nutrient concentration. To calculate the freshwater fraction of total SGD, a two endmember mixing analysis is employed using a system of two equations and two unknowns:

$$1 = f_O + f_{GW} \quad (3)$$

$$S_m = S_O f_O + S_{GW} f_{GW} \quad (4)$$

where f_O is the oceanic fraction of SGD, f_{GW} is the fresh groundwater fraction, S_{GW} is the salinity of groundwater measured in supply wells proximal to the field area, S_O is the salinity of the marine endmember, assumed to be 35.5 ppt, and S_m is the salinity measured in coastal groundwater samples collected from beachface seeps and piezometers. Fresh SGD fractions are calculated using the mean salinity measured in all coastal groundwater samples from a particular field area. Beachface seep and piezometer samples were collected within three hours of low tide and thus are biased towards low tide coastal groundwater salinities.

4. Results

4.1 Land Use

Land use transected by coastal groundwater samples includes developed land, undeveloped land, OSDS, sugarcane, pineapple, unspecified agriculture, and dairy farms. Fig. 4 illustrates the mean type of land use transected by all coastal groundwater samples for each

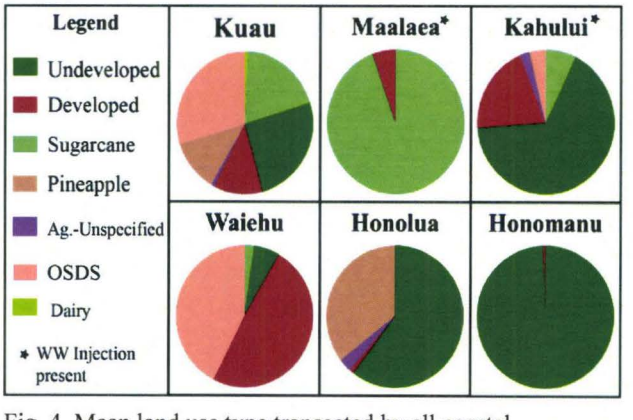

Fig. 4. Mean land use type transected by all coastal groundwater samples from each field area. Asterisks indicate areas that also contain wastewater injection wells.

field area. Honomanu and Maalaea flowpaths transect principally (>90%) undeveloped land and sugarcane, respectively, while the other field areas are more mixed. The dominant type of land use transected by flowpaths at each of the field areas are: Kuau - 30% OSDS, Maalaea - 94% sugarcane, Kahului – 66% undeveloped, Waiehu – 49% developed, Honolua – 60% undeveloped, and Honomanu - 99% undeveloped.

4.2 Salinity

Well samples had the lowest salinities and ranged from 0.05 – 0.40 (mean = 0.20, s.d. = 0.12), coastal groundwater sample had the largest range in salinities from 0.10 - 32.49 (mean = 7.24, s.d. = 8.00), and coastal surface water samples salinities ranged from 20.70 - 35.83 (mean = 32.86, s.d. = 3.16). Coastal water samples generally had lower salinities closer to shore showed significant correlation between distance from shore and salinity at 4 of the 6 sites using Spearman's Rank correlation. Sample type, field locations, latitude, longitude, salinity, and dissolved oxygen saturation are shown in appendix A1.

4.3 Groundwater and Coastal Water Nutrient Concentrations

Coastal groundwater, wells, and springs had highest N+N, Si, PO_4^{3-}, and NH_4^+ concentrations while nutrient concentrations in coastal surface water samples were much lower. Groundwater concentrations ranged from 0.02 μM to 460 μM for N+N, 0 to 115 μM for NH_4^+, 0.28 to 8.53 for PO_4^{3-}, and 54 to 899 for Si. Coastal water concentrations ranged from 0 to 59.6 μM for N+N, 0 to 4.8 for NH_4^+, 0 to 4.1 μM for PO_4^{3-}, and 0 to 518 μM for Si. NH_4^+ was at or near detection for many samples. Mean coastal water nutrient concentrations are given in Table 2 and nutrient concentrations for all samples are in appendix A2.

Table 2. Mean coastal surface water nutrient concentrations. Standard deviations, number of samples (n), and salinity ranges for each field area are shown.

Site	n	Salinity	PO_4^{3-}	Si	N+N	NH_4^+
Kuau	12	28.01 - 35.71	0.31 ± 0.26	68 ± 53	23 ± 17	0.26 ± 0.34
Maalaea	22	28.51 - 35.85	0.19 ± 0.29	28 ± 34	12 ± 18	0.77 ± 1.1
Kahului	25	30.03 - 34.88	0.40 ± 0.81	78 ± 101	3.1 ± 4.3	0.33 ± 0.90
Honolua	16	30.26 - 35.02	0.09 ± 0.11	41 ± 29	1.4 ± 1.5	0.57 ± 1.0
Waiehu	13	20.70 - 35.35	0.11 ± 0.23	34 ± 37	0.06 ± 0.07	0.55 ± 1.2
Honomanu	11	32.52 - 34.74	0.24 ± 0.14	51 ± 30	0.18 ± 0.24	0.12 ± 0.26

We examined correlations between distance from shore and nutrient concentration in coastal water samples using Spearman's rank correlation. Coastal water PO_4^{3-}, Si, and N+N were significantly ($p < 0.05$) inversly correlated with distance from shore at 4 of 6 field sites. Honomanu did not display a significant inverse realtionship between distance from shore and any of the nutrient species in coastal water samples and NH_4^+ was not significantly correlated with distance from shore at any of the field areas.

Linear regressions on N+N, PO_4^{3-}, and Si versus salinity for all coastal surface water and coastal groundwater samples for each field area were all statistically significant ($\rho < 0.05$) and are shown in Fig. 5. Regressions on NH_4^+ were not statistically significant. These regressions (Fig. 5) were used to determine groundwater endmember concentrations, shown in Table 3. The alternative method to determine the groundwater endmember concentration would be to salinity unmix all samples using Equation 1 and then find the mean of all unmixed groundwater concentrations from a particular field area. Because regressions on nutrient concentration and O isotopic composition of water versus salinity were mostly significantly linear ($p<0.01$), except for ammonium, the linear unmixing equation is appropriate. The results of either method are quite similar and are shown in Table 3, though the regression method generally resulted in more conservative estimates.

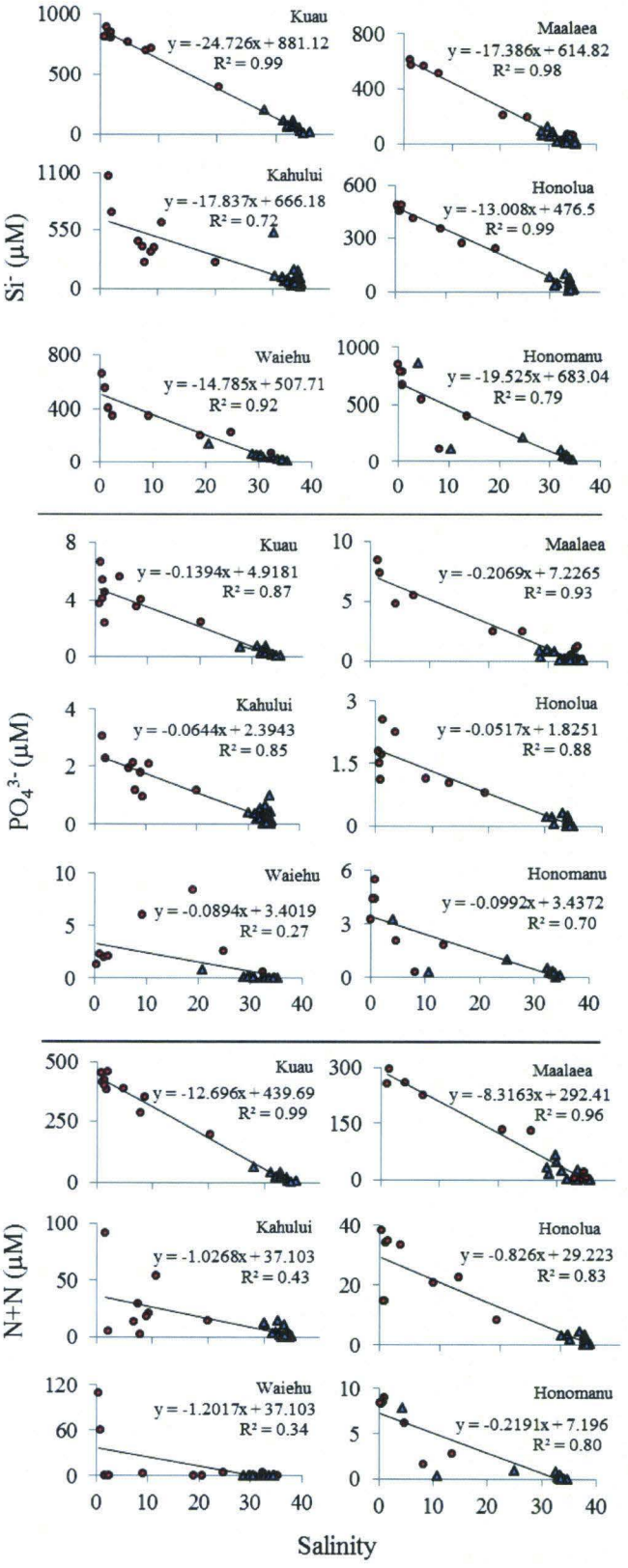

Fig. 5. N+N, PO_4^{3-}, and Si vs. salinity used to derive coastal groundwater endmember values. Coastal groundwater samples are red circles and marine surface samples are blue triangles. Regression equations, best fit line, and coefficient of determination are shown. All regression are significantly linear at $p<0.01$ except for Waiehu PO_4^{3-}, where $p = 0.02$.

Table 1. Coastal groundwater nutrient concentrations. Groundwater endmember concentrations are shown on the left with the standard error of the estimate indicated after the ± symbol. Mean, salinity-unmixed, coastal groundwater concentrations are shown on the right with the standard deviation shown after the ± symbol and the number of samples indicated by the *n* column. Asterisks indicate the number of samples used in the mean calculation if nutrient concentrations in some samples were non-detectable.

	Coastal groundwater endmember concentrations (μmol L^{-1})				Mean salinity unmixed coastal groundwater concentrations (μmol L^{-1})				
Site	**PO_4^{3-}**	**Si**	**N+N**	**NH_4^+**	**n**	**PO_4^{3-}**	**Si**	**N+N**	**NH_4^+**
Kuau	4.9 ± 0.8	884 ± 27	439 ± 22	0.9 ± 1.0	10	5.0 ± 1.3	889 ± 44	440 ± 35	1.7 ± 3.1
Maalaea	7.2 ± 0.6	611 ± 27	291 ± 17	0.4± 1.0	6	7.2 ± 1.4	609 ± 65	322 ± 70	0.3 ± *[5]0.6
Kahului	2.4 ± 0.3	664 ± 132	55 ± 19	†1.8 ± 1.9	9	2.4 ± 0.6	625 ± 250	36 ± 31	41 ± *[4]62
Honolua	1.8 ± 0.3	473 ± 24	29 ± 5.6	0.6 ± 1.0	9	1.8 ± 0.5	475 ± 30	29 ± 10	1.2 ± 1.0
Waiehu	2.5 ± 2.0	505 ± 59	37 ± 24	2.6 ± 1.4	8	6.7 ± 5.9	601 ± 225	33 ± *[7]41	1.5 ± *[6]2.6
Honomanu	3.4 ± 1.0	681 ± 153	7.9 ± 1.7	0.8 ± 0.8	7	3.3 ± 1.7	647 ± 236	7 ± 3	1.3 ± 1.8

* indicates the number of samples used in the mean calculation

† Sample KWP-5 was omitted from the endmember calculation because of the anomalously high NH_4^+ concentration of 118.3 μM.

4.4 H and O Isotopic Compositions of Water

A strong linear correlation exists between the oxygen isotopic composition of water and salinity for all groundwater and coastal water samples (Fig. 6). The $\delta^{18}O$ of water in coastal water samples ranged from -3.8 to 0.2‰ and had a mean of -0.4‰, coastal groundwater samples had values ranging from -4.6‰ to 0.2‰ with a mean of -2.9‰, well samples had $\delta^{18}O_{H2O}$ ranging from -5.4 to -2.8‰ with a mean of -4.0‰. O isotopic compositions in all samples are shown in appendix A2.

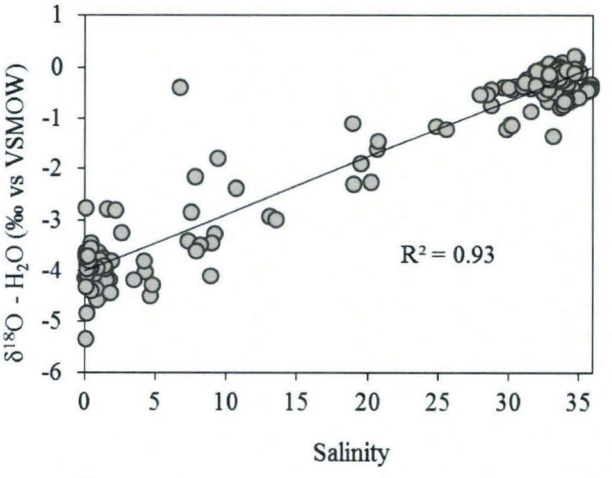

Fig. 6. $\delta^{18}O$ versus salinity for all groundwater and coastal water samples collected during this study ($r^2 = 0.97$, $y = 0.11x - 4.01$).

4.5 N and O Isotopic Compositions of Nitrate

$\delta^{18}O_{NO3}$ vs. $\delta^{15}N_{NO3}$ values for combined coastal groundwater and coastal surface water samples from each field area along with a sample of treated wastewater effluent from Kahului wastewater treatment facility are shown in Fig. 7 and appendix A2. $\delta^{15}N_{NO3}$ and $\delta^{18}O_{NO3}$ values from all samples collected

ranged from 0.3– 44.1‰ for N and -3.8 – 22.6‰ for O. Highest mean $\delta^{15}N_{NO3}$ values were from the Kahului field area (18.3‰), and the lowest mean values were from Honomanu (1.4‰).

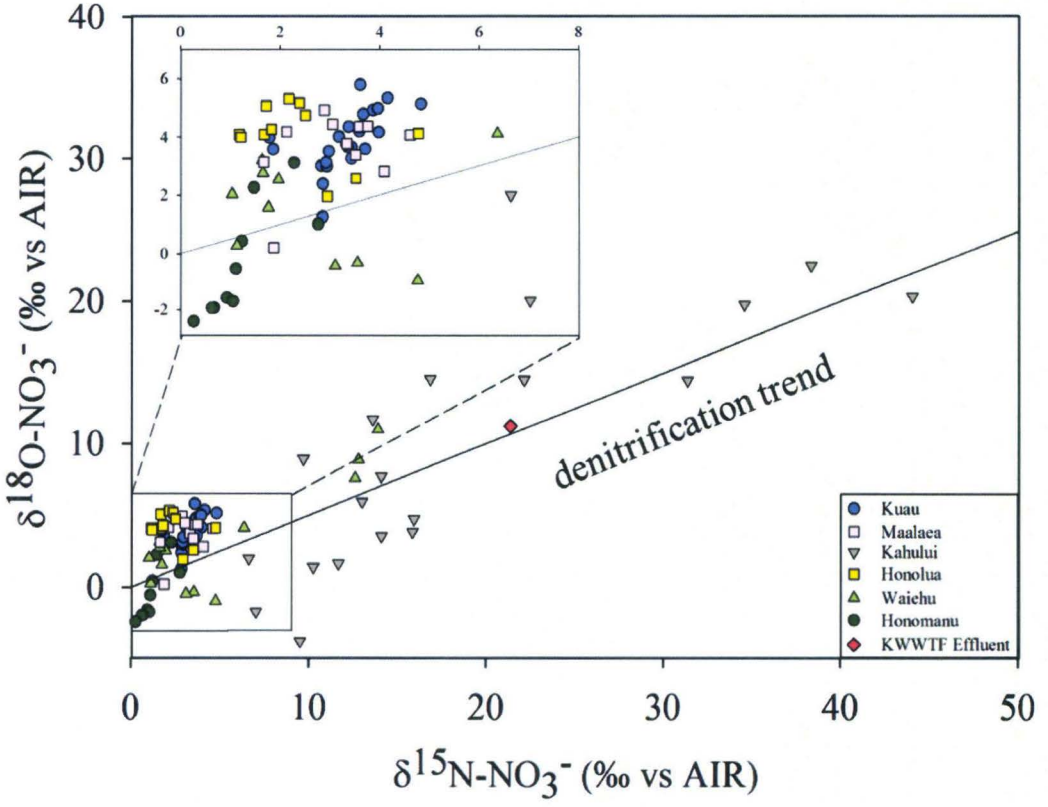

Fig. 7. $\delta^{18}O_{NO3}$ vs. $\delta^{15}N_{NO3}$ for all coastal water and coastal groundwater samples collected from each field area. The Kahului Wastewater Treatment Facility effluent sample composition is shown as a red diamond. Inset plot is a large scale subset.

4.6 Multiple Regression on Land Use and Groundwater Nutrient Concentration

Regression was run on all land use variables initially, then re-run using only the statistically significant ($\rho < 0.05$) variables from the initial regression; results presented reflect only analysis conducted on statistically significant independent variables. Regression equations with standardized coefficients are shown in Table 4. The regression on N+N had the highest R^2 value (0.81), was statistically significant ($F[4, 61] = 66.693$, $\rho < 0.001$), and sugarcane and unspecified agriculture are the most significant independent variables ($\rho < 0.001$) followed by pineapple ($\rho = 0.006$) and undeveloped land ($\rho = 0.01$). A

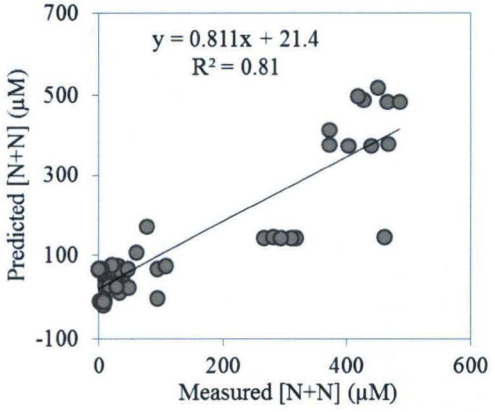

Fig. 8. N+N concentration predicted from multiple regression equation versus measured N+N concentration.

plot of the predicted versus measured N+N concentration is shown in Fig. 8. The regression on Si and PO_4^{3-} had R^2 values of 0.28 and 0.07; the regression on PO_4^{3-} was not significant. NH_4^+ was excluded in this analysis because of low and highly variable concentrations in groundwater samples. Regression residuals for all three nutrient species failed the Kolmogorov-Smirnov normality test, though q-q plots for N+N (not shown) indicate that the deviation from normality is not severe. Furthermore, regression analysis is quite robust against violations of normality and thus significance tests can still be performed even when this assumption is violated (Berry and Feldman, 1985). Adherence to assumptions of homoscedasticity and linearity were investigated using plots of residuals versus predicted values and residuals versus independent variables (not shown), respectively; these assumptions were not violated for any of the regressions.

Table 4. Multiple regression equations and R^2 values for various nutrient species. Regression intercepts are indicated by the bold β symbol, independent land use type and dependent nutrient species are also bolded, and standardized coefficients are shown.

Regression Equation	R^2
[N+N] = 68.2**β** + 1.32**Sugarcane** + 0.02**Pineapple** – 0.17**Undeveloped** – 0.95**Unspecified Ag.**	0.81
[Si] = 45.1**β** + 0.83**OSDS** - 0.26**Unspecified Ag.**	0.29
[PO_4^{3-}] = 3.67**β** + 0.4**Sugarcane** – 0.37**Unspecified Ag.**	0.07

4.8 Radon Stationary Time Series

^{222}Rn activity measured in surface coastal waters during time series ranged from 0.06 to 18.3 dpm/L, salinity ranged from 2.59 to 34.82, and mixed salinity layer plume thickness varied from 0 to 139 cm (Fig. 9). SGD plume thickness and salinity are generally well correlated with each other and ^{222}Rn activity is inversely correlated. This is expected because salinity increases on a rising tide, the rising tide

decreases the hydraulic gradient, groundwater discharge is reduced, and radon activity gets diluted by the larger incoming water mass.

SGD fluxes were normalized by the shore parallel length of the model polygon side in order to present discharge rates in terms of discharge volume per meter of shoreline per day. Important model parameters used in stationary time series SGD flux calculations are shown in Table 5. SGD fluxes calculated during a 30 minute collection cycle ranged from 0 to 29.3 $m^3/m/d$ for both total (fresh + saline) and fresh SGD. Mean SGD fluxes over an entire time series ranged from 1.1 to 6.9 $m^3/m/d$ for total SGD. Fresh SGD fluxes were calculated using the minimum, maximum, and mean coastal groundwater salinities measured in beach face seeps and piezometers and as such we present a range of possible fresh fluxes, depending on the coastal groundwater endmember salinity used. Fresh SGD calculated using mean coastal groundwater salinity ranged 0.1 to 6.7 $m^3/m/d$ (Table 6). Raw radon time series data is shown in appendix A3.

Table 5. Time series model parameters and measurements. Time series locations, mixed salinity layer depths measured during depth profiling, surface area of radon model box, and shore parallel box side lengths are shown. ^{222}Rn activity are mean values measured over an entire time series, while the standard deviations represent the tidally modulated variance that occurs over the duration of the time series.

Field Area	Latitude	Longitude	Depth (cm)	Surface Area (m^2)	Length of Shoreline (m)	Mean ^{222}Rn activity (dpm/L)
Kuau	20.92622	-156.37012	65	2568	105	11.6 ± 3.9
Maalaea	20.79177	-156.50947	75	4172	61	9.6 ± 3.1
Kahului	20.89699	-156.45493	99	1434	100	1.1 ± 0.6
Honolua	21.01325	-156.63942	35	414	41	9.0 ± 4.2
Waiehu	20.91541	-156.49156	63	4643	217	0.6 ± 0.2
Honomanu	20.86082	-156.16530	77	2507	108	6.1 ± 2.8

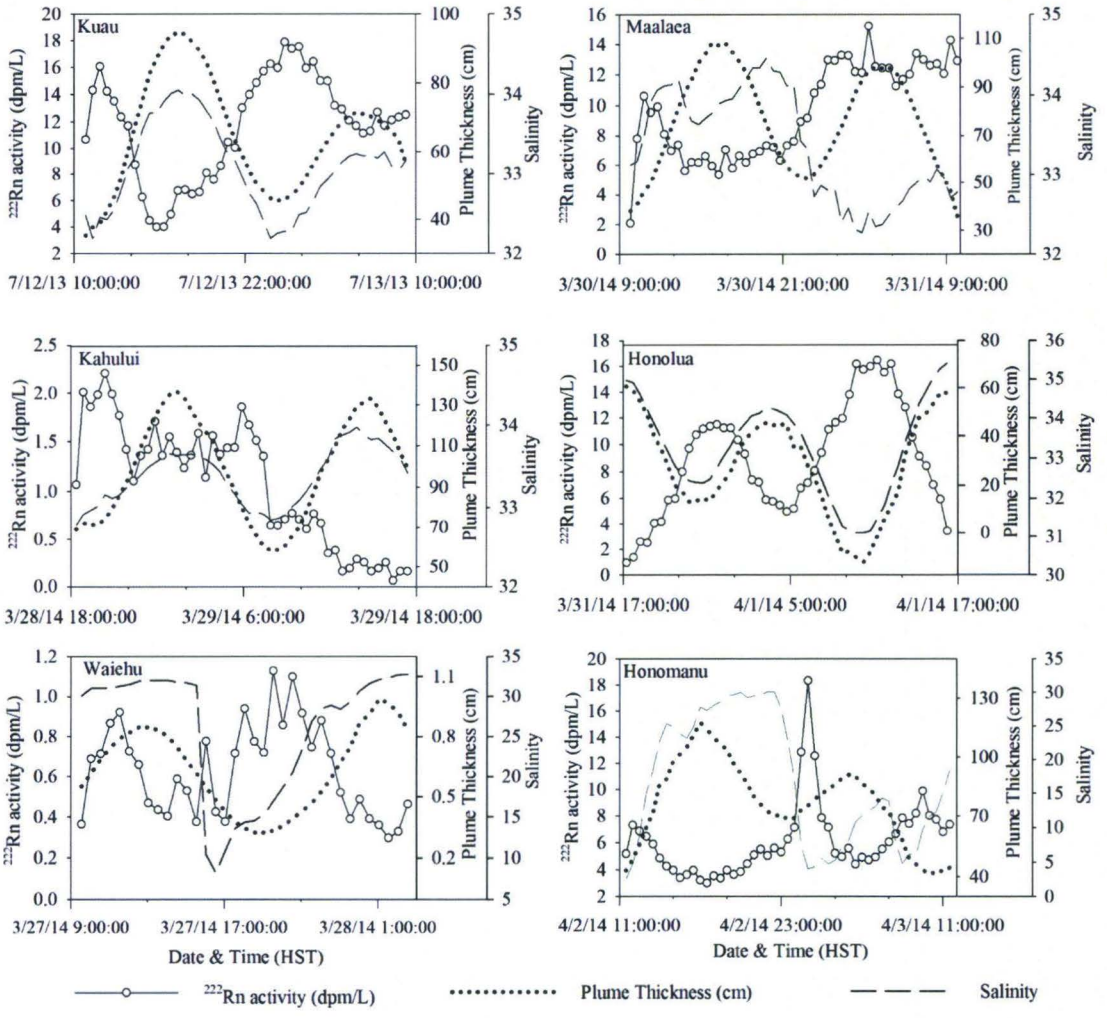

Fig. 9. 222Rn activity, salinity, and mixed fresher layer SGD plume thickness measured at each coastal water stationary radon time series deployment. Individual ^{222}Rn measurements are shown as white circles, salinity as dashed lines, and plume thickness as black dots. Vertical scale varies from plot to plot in order to optimally display the full range of data.

Table 6. Total and fresh SGD fluxes calculated from stationary radon time series data. The mean salinity of coastal groundwater (CGW) samples used to calculate the fresh SGD fraction is shown along with the standard deviation, and the number of samples used in the mean calculation in parenthesis. For the fluxes, standard deviations are indicated after the ± symbol and represent the tidally modulated variance that occurs over the duration of the time series.

Field Area	Mean Total SGD flux ($m^3/m/day$)	Mean CGW salinity	Fresh SGD flux ($m^3/m/day$)
Kuau	5.1 ± 2.8	5.0 ± 6.1 (10)	4.4 ± 2.5
Maalaea	6.9 ± 3.4	22.2 ± 14.5 (12)	2.6 ± 1.3
Kahului	1.1 ± 0.4	8.2 ± 5.1 (9)	0.8 ± 0.3
Honolua	3.3 ± 1.9	4.9 ± 6.7 (10)	2.4 ± 1.4
Waiehu	1.1 ± 0.5	12.8 ± 12.7 (7)	0.7 ± 0.4
Honomanu	6.6 ± 6.1	4.1 ± 4.7 (8)	5.8 ± 5.4

4.9 Radon Surface Water Surveys

While the radon time series provides a good estimate for average SGD over a tidal cycle, it does not provide information on the spatial distribution and heterogeneity of SGD. This can be studied by radon surface water survey SGD fluxes calculated at each field area and are shown in Fig. 10. The multicolored lines indicate the path the boat traveled and the color gradient indicates the magnitude of SGD flux. Important parameters used in the SGD fluxes along with the calculated fluxes are shown in Table 7. Radon surface water survey SGD fluxes are used to scale the time series calculated fluxes. The mean ratio of the radon survey flux calculated at the time series location relative to the survey flux at every other location along each shoreline transit is included in Table 7. In the discussions that follow we further proportion these scaled time series flux rates between total (fresh + marine) and freshwater only SGD fractions, and refer to them as either scaled total or scaled fresh SGD for the remainder of the text below. Radon surface water survey data is shown in appendix A4.

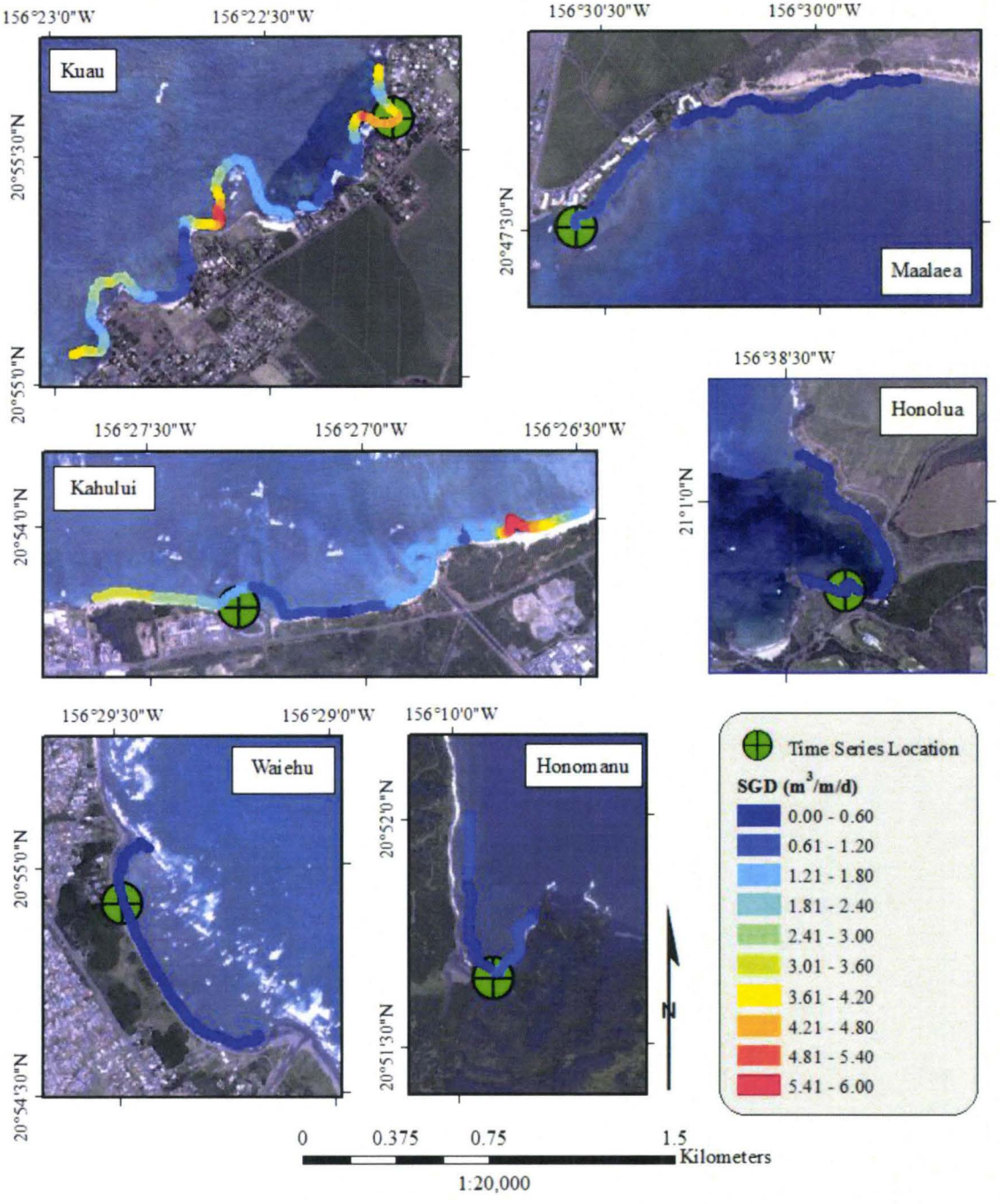

Fig. 10. Surface water radon survey fluxes. Total SGD fluxes (m3/m/d) calculated from radon surface water surveys at each field area. The location of the radon time series station is indicated by the green circle

Table 7. Radon surface water survey parameters and SGD fluxes. The mean and standard deviation for select parameters used in radon surface water survey SGD flux calculations as well as the calculated fluxes are shown. The standard deviation represent the variance that occurred along the entire survey at a particular area. The last column shows the mean ratio of the survey flux calculated for each coastal polygon relative to the survey flux calculated for the coastal polygon at the time series location.

Field Site	Sal.	Depth (m)	^{222}Rn activity (dpm/L)	SGD (m^3/day)	SGD (m^3/m/day)	Discharge relative to TS location
Kuau	34.35 ± 0.34	0.7 ± 0.2	3.0 ± 1.4	340 ± 260	2.3 ± 1.7	0.86 ± 0.68
Maalaea	33.60 ± 1.8	0.3 ± 0.3	9.2 ± 4.8	53 ± 74	0.5 ± 0.4	1.6 ± 1.9
Kahului	32.39 ± 0.45	1.6 ± 0.4	2.4 ± 1.0	450 ± 308	2.1 ± 1.6	1.4 ± 0.97
Honolua	34.82 ± 0.20	0.7 ± 0.7	1.0 ± 0.6	14 ± 16	0.1 ± 0.1	1.8 ± 2.0
Waiehu	31.91 ± 1.8	0.5 ± 0.3	0.7 ± 0.6	24 ± 29	0.2 ± 0.2	0.79 ± 1.0
Honomanu	32.00 ± 2.2	1.4 ± 0.5	3.1 ± 1.9	131 ± 57	0.6 ± 0.3	0.50 ± 0.15

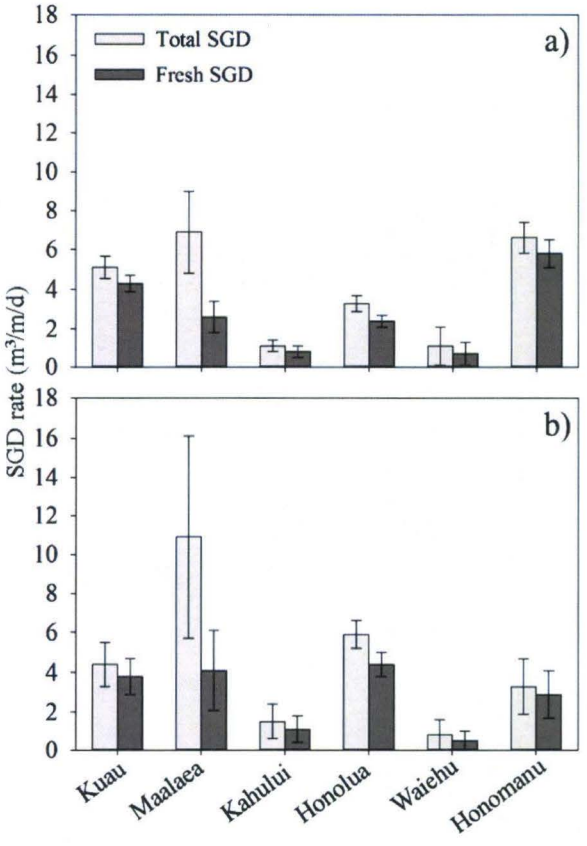

Fig. 11. SGD fluxes at each field area. Stationary time series fluxes (a) and scaled SGD fluxes (b). Error bars are the propagated uncertainty associated with the flux calculation.

4.10 SGD Rates and Nutrient Fluxes

SGD fluxes calculated at the time series location and scaled SGD fluxes are shown in Fig. 11a and b, respectively, along with the uncertainty associated with the measurement. Nutrient fluxes for a particular field area are shown in Table 9 and were determined by multiplying the groundwater endmember nutrient concentration (Table 3) by the scaled fresh SGD flux (Table 8). Uncertainties associated with the nutrient flux measurements are presented in Table 9. Nutrient fluxes for NH_4^+ were not calculated because of the large uncertainty associated with calculating the

NH_4^+ endmember. For the discussion, all references to nutrient fluxes will be in regard to the flux calculated using the scaled fresh SGD.

Table 8. Scaled total and scaled fresh SGD rates at each of the field areas. Fluxes presented are mean flux calculated over a tidal cycle. Standard deviations are indicated after the ± symbol and represent the tidally modulated variance that occurs over the duration of the time series. The error is the propagated uncertainty associated with the calculated flux.

	Scaled Total SGD (m^3/m/d)	Error	Scaled Fresh SGD (m^3/m/d)	Error
Kuau	**4.4 ± 2.4**	1.1	**3.8 ± 2.1**	0.9
Maalaea	**10.9 ± 5.4**	5.2	**4.1 ± 2.0**	2.0
Kahului	**1.5 ± 0.6**	0.9	**1.1 ± 0.5**	0.7
Honolua	**5.9 ± 3.3**	0.7	**4.4 ± 2.5**	0.6
Waiehu	**0.8 ± 0.4**	0.8	**0.5 ± 0.3**	0.5
Honomanu	**3.3 ± 3.1**	1.4	**2.9 ± 2.7**	1.2

Table 9. Nutrient fluxes. Nutrient fluxes were determined for scaled fresh SGD rates. Standard deviations are indicated after the ± symbol and represent the tidally modulated variance that occurs over the duration of the time series. The error is the propagated uncertainty associated with the calculated nutrient fluxes.

Field area	PO_4^{3-} (mmoles/m/d)	error	Si (mmoles/m/d)	error	N+N (mmoles/m/d)	error
Kuau	**19 ± 10**	5.4	**3361 ± 1857**	802	**1666 ± 920**	403
Maalea	**30 ± 14**	14	**2506 ± 1222**	1228	**1192 ± 581**	586
Kahului	**2.6 ± 1.2**	1.7	**730 ± 331**	487	**61 ± 28**	44
Honolua	**8.0 ± 4.5**	1.6	**2081 ± 1182**	303	**128 ±73**	30
Waiehu	**1.3 ± 0.8**	1.6	**252 ± 151**	254	**18 ± 11**	22
Honomanu	**9.9 ± 9.2**	5.0	**1974 ± 1837**	929	**23 ± 21**	11

5. Discussion

5.1 Nutrient Trends in Groundwater and Coastal Waters

Ocean waters surrounding Hawai'i are oligotrophic and the majority of nutrients to coastal waters are supplied by terrestrial sources. Groundwater nutrient input likely driving observed coastal water nutrient concentrations as evidenced by the fact that field areas with high groundwater endmember N+N and Si

concentrations also have high mean N+N and Si coastal water concentration and vice-versa. Furthermore, N+N, PO_4^{3-}, and Si are significantly inversely linearly correlated with distance from shore at most field areas. Coastal water nitrate is terrestrial in origin as evidenced by similarity between coastal water and coastal groundwater $\delta^{15}N$ and $\delta^{18}O$ values from a particular field area, except at Kahului, which is discussed below. Stream water was discharging at both Waiehu and Honomanu and thus stream input cannot be discounted as a source of nutrients at those sites. However, stream nutrient concentrations at these two sites were low, particularly for N+N (< 2 μM) and coastal water nutrient concentrations were low relative to other areas, suggesting neither streams nor groundwater are substantial sources of nutrients to coastal waters. The four other areas studied did not have stream inputs and were not sampled during rain events so nutrient contribution from streams or runoff is unlikely, particularly because residence times measured on south Maui coastal waters, though not at our field sites, ranged between 1 and 6 hours (Herzfeld, 2011). Tables 2 and 3 show that mean coastal water and groundwater endmember N+N concentrations vary considerably among the field areas, by factors of 383 and 55, respectively, while the other species vary by less than a factor of 5. The important implication of this result is that it suggests that land use has a substantial effect on N+N concentrations, and a much smaller effect on the other nutrient species

5.2 Application of multiple regression modeling to nutrient source identification

The results of our regression analysis of land use types (Table 4) suggests that for sites studied on Maui sugarcane contributes the greatest amount of N+N to groundwater, followed by pineapple. These results are consistent with the results from $\delta^{15}N$ values of dissolved nitrate, discussed below. In contrast, undeveloped land and unspecified agriculture have an inverse relationship with N+N. Undeveloped lands results suggest a lack of anthropogenic sources and little N is contributed to groundwater in these areas. The inverse relationship between N+N and unspecified agriculture is difficult to explain.

5.3 Sources of Nutrients to the Field Areas

5.3.1 Undeveloped Land (Honomanu)

Lowest N+N coastal groundwater endmember concentrations occurred at Honomanu Bay where groundwater flows beneath almost exclusively (99%) undeveloped land (Fig. 4). Coastal water N+N concentrations at Honomanu were also very low (Table 2) reflecting the low groundwater endmember concentration. Mean $\delta^{15}N$ and $\delta^{18}O$ isotopic compositions are also lowest at Honomanu, suggesting that the nitrite in this field area is primarily coming from soils or atmospheric deposition. Honomanu thus represents a baseline endmember by which N+N concentrations from other areas can be compared.

5.3.2 Commercial Agriculture and OSDS (Kuau)

At Kuau, groundwater flowpaths are overlain by a number of different land use types (Fig. 4) including pineapple, sugarcane, and OSDS, making identification of nutrient sources difficult. To discriminate nitrate contributions in this area we examined changes in $\delta^{15}N$ values and nitrate concentration along groundwater flowpaths. Upslope of the Kuau coastal field area we sampled three public water supply wells (Fig. 12A). Groundwater head contours approximately parallel elevation contours and thus down-gradient groundwater flows roughly downhill. As shown in Fig. 12A, groundwater NO_3^- concentration increases down-gradient from 29 μM at KW to 94 μM at HW, while $\delta^{15}N_{NO3}$ values are effectively unchanged. The increase in NO_3^- concentration occur as groundwater transects land use that includes a large area with a high density of septic systems and lesser amounts of undeveloped land, developed land, and pineapple. Because $\delta^{15}N$ values do not change, the $\delta^{15}N$ of the 65 μM of added nitrate must also have a $\delta^{15}N$ of around 4‰. This value is consistent with values expected from soil, air, and fertilizer-derived nitrate, and too low for the 10 – 20‰ expected from an OSDS source (McMahon and Böhlke, 1996; Kendall et al., 1998). Further upslope PW well has a lower $\delta^{15}N$ value and thus there is an increase in $\delta^{15}N$ values from the PW well to HW well. Assuming the 71 μM increase in NO_3^- is from a single source we can use a 2-component isotope mass balance to estimate the $\delta^{15}N$ value of the NO_3^- added:

$$94 * \delta^{15}N_{HW} = 23 * \delta^{15}N_{PW} + 71 * \delta^{15}N_{added} \quad (5)$$

where 94, 23, and 71 are the concentration of NO_3^- at HW, PW, and HW - PW, respectively, $\delta^{15}N_{HW}$ = 4.0‰, $\delta^{15}N_{PW}$ = 2.9‰, and $\delta^{15}N_{added}$ is the isotopic composition of the NO_3^- added. Solving for $\delta^{15}N_{added}$ yields a value of 4.3 ± 1.4 ‰, well below the 10 – 20‰ value expected for OSDS nitrate. The important implication of these analyses is that while groundwater flows beneath this high density OSDS area, $\delta^{15}N$ values do not suggest that OSDS nitrate is added.

An examination of coastal groundwater samples at Kuau reveals that the mean NO_3^- concentration that in these samples is 345 μM higher than the nearest upgradient well (HW; Fig. 12B). The increase in NO_3^- concentration between well HW and the coast occurs as groundwater leaves the high density septic area and flows beneath pineapple and sugarcane fields (Fig. 12A). $\delta^{15}N$ values decrease from well HW to the coast. Using a two component isotope mass balance equation we can estimate the $\delta^{15}N$ of the added NO_3^-:

$$439 * \delta^{15}N_{CGW} = 94 * \delta^{15}N_{HW} + 345 * \delta^{15}N_{added} \quad (6)$$

where 439, 94, and 345 are the concentrations of mean coastal groundwater (CGW), HW, and the nitrate added from HW to CGW, $\delta^{15}N_{CGW}$ = 2.9‰, $\delta^{15}N_{HW}$ = 4.0 ‰, and $\delta^{15}N_{added}$ is the isotopic composition of the nitrate added. Solving for $\delta^{15}N_{added}$ yields a value of 2.6 ± 1.1‰. The urea fertilizer applied to sugarcane and pineapple fields (Falconer, 1991) converts to nitrate with a typical $\delta^{15}N$ value of around 0 ± 1.3 ‰ and average soil nitrate $\delta^{15}N$ produced from fertilizer is 4.3 ‰ (Kendall, 1998, Böhlke, 2003). The $\delta^{15}N$ value calculated for the nitrate added is similar to the values of both urea derived nitrate and soil nitrate produced from fertilizer (Kendall, 1998). Thus, mixing of low $\delta^{15}N$ nitrate derived from urea fertilizers with background groundwater that has a $\delta^{15}N$ of around 4.0 ‰ is the likely explanation for the observed decrease in isotopic composition and 345 μM increase in nitrate concentration between the lowest elevation well and the coast. Although $\delta^{15}N$ values around 2.6‰ can be produced by soils and the atmosphere, the large increase in nitrate concentration occurring as groundwater flows beneath sugarcane

and pineapple fields suggest a fertilizer source. Because nitrate comprises greater than 99% of the N+N concentration in each of the samples collected at Kuau we calculate that commercial agriculture is adding ~78% of the 440 μM coastal groundwater endmember N+N.

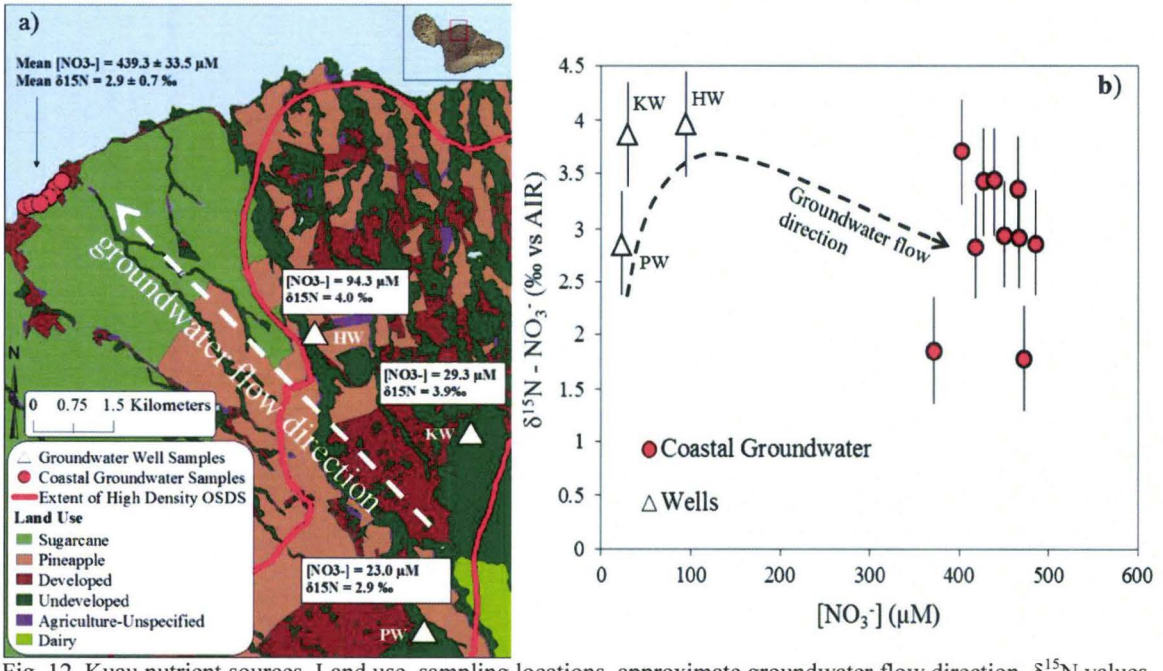

Fig. 12. Kuau nutrient sources. Land use, sampling locations, approximate groundwater flow direction, $\delta^{15}N$ values, and nitrate concentrations are shown on the left. Binary plot on the right shows change in $\delta^{15}N$ and NO_3^- concentration along the groundwater flowpath. The 71 μM of nitrate added to groundwater in the high septic density area has $\delta^{15}N$ values inconsistent with an OSDS source. As groundwater flow exits the high septic density, flows beneath sugarcane and pineapple fields, and finally reaches the coast $\delta^{15}N$ values decrease by 1‰ and NO_3^- increases by 345 μM; the $\delta^{15}N$ value of 345 μM of NO_3^- added is consistent with a fertilizer source.

5.3.3 Appraisal of Wastewater Injection (Kahului)

5.3.3.1 Three endmember mixing analysis

Kahului Wastewater treatment Facility (KWTF) injects approximately 4 million gallons per day of treated effluent (Scott Rollins, KWTF, personal communication; Dailer et al., 2010) through 8 injection wells less than 50 meters from the coast. Using $\delta^{18}O_{H2O}$ values and salinity we conducted a two component, three endmember mixing analysis to determine if this effluent was present in coastal groundwater. Salinity and $\delta^{18}O_{H2O}$ values are appropriate tracers for this kind of analysis because both exhibit conservative chemical behavior (Fig. 6) and all three endmembers have different concentrations and

compositions for each of the tracers. In this model we assume that the chemical composition of coastal groundwater samples is a combination of upland groundwater, coastal water, and injected effluent, whereby endmembers used in this analysis are water from PW public drinking water supply well, the mean coastal water isotopic composition and salinity of all coastal water samples collected from coastal waters at Kahului (n = 22), and wastewater effluent obtained from the KWTF. Fig. 13A illustrates how the nine Kahului coastal groundwater samples plot relative to these endmembers. Samples within the endmember triangle shown in Fig. 13A are comprised entirely of some proportion of these endmembers, while samples that plot outside the triangle cannot be satisfactorily explained by the model compositions alone. Five of the nine coastal groundwater samples collected at Kahului do not fall within the mixing triangle. However, because four of the five samples that plot outside the triangle plot quite close to the triangle edges, and are clustered around the effluent endmember, we suspect that the endmembers chosen are correct, but that the single effluent sample we are using as the effluent endmember is not capturing the full variability in chemical composition. Similar investigations of the Lahaina Wastewater Treatment Facility on west Maui (Hunt and Rosa, 2009; Glenn et al., 2012 and 2013) for example, have shown that the $\delta^{18}O_{H2O}$ values and salinity of the injected effluent is temporally variable and it is thus possible that the single sample is not completely representative of the bulk composition of effluent injected into the aquifer.

The ternary diagram (Fig. 13B) is used to show the proportion of each endmember in a sample after calculating relative fractions. The fraction of each end member was calculated by simultaneously solving a system of three equations and three unknowns:

$$1 = f_m + f_{GW} + f_{eff} \quad (7)$$

$$S_{KWP} = S_m f_m + S_{GW} f_{GW} + S_{eff} f_{eff} \quad (8)$$

$$\delta^{18}O_{KWP} = \delta^{18}O_m f_m + \delta^{18}O_{GW} f_{GW} + \delta^{18}O_{eff} f_{eff} \quad (9)$$

where *f* is the fraction of each end-member, *S* is salinity, $\delta^{18}O$ is the oxygen isotope composition of water, the subscripts *m*, *GW*, and *eff* are for the marine, groundwater, and effluent end-members, respectively,

and the subscript *KWP* is for the sample being evaluated. The results of the mixing analysis using PW well $\delta^{18}O$ values show that the four groundwater samples within the mixing triangle range in their end-member compositions from 12-53% marine, 4-44% upland groundwater, and 26-75% effluent (Fig. 13B).

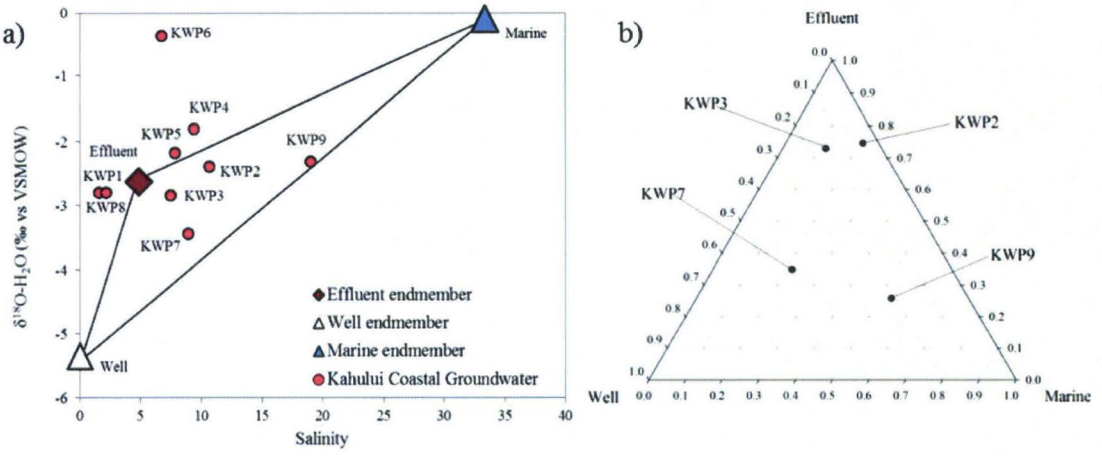

Fig. 13. Three-component mixing analysis of the contribution of wastewater injection to coastal groundwater. A) The three component mixing model endmembers that mix to form Kahului coastal groundwater are PW well (white triangle), mean marine surface water from Kahului (blue triangle) and Kahului Wastewater Treatment Facility effluent (red diamond). Red circles are coastal groundwater samples from the Kahului field area and the sample names are shown. Black lines are conservative mixing lines between two of the end-members. Samples that plot within the mixing triangle are comprised entirely of some proportion of the three end-members while samples that plot outside do not fit in the model. B) Ternary diagram shows the proportion of each endmember that mixed to form the coastal groundwater samples that lie within the mixing triangle from A).

5.3.3.2 N and O Isotopic Composition of Dissolved Nitrate

$\delta^{15}N$ and $\delta^{18}O$ values of dissolved nitrate suggest wastewater effluent is discharging to groundwater and coastal water at Kahului. N and O isotopic composition of dissolved nitrate have been used extensively to identify sources and transformations of NO_3^- in groundwater and marine systems (Kendall, 1998; Böhlke, 2003; Singleton et al., 2005; McMahon and Böhlke, 2006; Wankel et al., 2006; Hunt and Rosa, 2009; Kaushall et al., 2011; Glenn et. al., 2012, Lapworth et al., 2013). The sample of treated effluent collected from KWTF had $\delta^{15}N$ and $\delta^{18}O$ values of 21.4‰ and 11.3‰, respectively, which are consistent with values expected for treated sewage and are similar to effluent values measured at other municipal wastewater treatment facilities on Maui (Hunt, 2007; Hunt and Rosa, 2009; Glenn et al., 2012). The wastewater treatment process used at Kahului includes simultaneous nitrification-denitrification to

attenuate N-species concentrations (County of Maui, 1990). This treatment ends after the denitrification phase, which leaves residual nitrate with $\delta^{15}N$ and $\delta^{18}O$ values that reflect the denitrification process. The samples from Kahului coastal groundwater and coastal surface waters had $\delta^{15}N$ values ranging from 7.0 to 44.1‰ (Fig. 7), with values on the high end of this range being consistent with nitrate-N that has been partially denitrified. Furthermore, many of the samples plot along a theoretical denitrification trend in which the isotopic enrichment of oxygen relative to nitrogen occurs in a ratio of approximately 1:2 (Kendall, 1998) (Fig. 7), suggesting that the nitrate in those samples have undergone partial denitrification, a phenomenon not observed in samples from any of the other field areas.

The $\delta^{15}N$ values observed in coastal groundwater samples collected from the Kahului field site bracket and cluster around the value of the effluent (Fig. 7), i.e. some values are lower and some are higher than the effluent. Samples with $\delta^{15}N$ values higher than the effluent sample contain nitrate that is derived from the wastewater injection facility but has continued to denitrify as it flowed through the aquifer, after injection. This has been observed by Glenn et al. (2012) at Lahaina for coastal water samples clearly fed in large part by Lahaina, Maui wastewater injection wells. These samples had NO_3^- concentrations that were low relative to other samples from Kahului (mean = 6.5 μM), as would be expected as a result of denitrification. By contrast, samples with $\delta^{15}N$ values lower than the effluent sample had NO_3^- concentrations that were generally higher (mean = 23.7 μM) than ^{15}N enriched samples, as would be expected from nitrate that has either mixed with another source and/or undergone lesser amounts of denitrification. All the samples that fall within the three endmember mixing triangle (Fig. 13A) had $\delta^{15}N$ values that were lower than the effluent, suggesting a mixture of effluent with low $\delta^{15}N$ background groundwater is the reason for the $\delta^{15}N$ values lower than the effluent endmember. The land use transected by Kahului coastal groundwater is most similar to land use transected by Kuau and Honolua (Fig. 4), areas with mean $\delta^{15}N$ values of 2‰ and 3.5‰, respectively, thus it is reasonable to expect the background groundwater nitrate at Kahului to have values in that range. Therefore, a mixture of background groundwater with a $\delta^{15}N$ of 2‰ to 3.5‰ and effluent with a $\delta^{15}N$ of ~22‰ could produce the values

between 7 and 22‰ observed some samples. While the high $\delta^{15}N$ values do not singularly identify wastewater as the nitrate source (e.g. Houlton et al., 2006) values upwards of 14‰ were not measured in any samples collected during this study, except for the samples from Kahului. This suggests that processes that may drive $\delta^{15}N$ and $\delta^{18}O$ towards high values are uncommon on Maui except in the presence of wastewater effluent.

5.3.4 Commercial Agriculture and Local Wastewater Injection (Maalaea)

The most likely sources of nutrients to coastal waters at Maalaea are sugarcane, which comprise 94% of the land use transected by groundwater flowpaths in the area, and localized, relatively small volume (0.15 MGD) wastewater injection wells at some of the beachside condominiums (Dollar et al. 2011). Our data are inconsistent with the presence of wastewater effluent because groundwater and coastal water $\delta^{15}N$ values are low (mean $\delta^{15}N$ = 3.13 ‰), NH_4^+ concentrations are low (mean = 0.71 μM), and dissolved oxygen concentrations are high (mean >100%). We were unable to collect background groundwater sample at Maalaea or an effluent sample from the coastal injection wells but we assume mean background groundwater $\delta^{15}N$ values at Maalaea are similar to Kuau (3.3‰), which has the most similar land use (Fig. 3). We also assume injection effluent $\delta^{15}N$ values at Maalaea condominiums is similar to that at Kahului wastewater treatment plant (21.38‰). If these assumptions are true, the mean $\delta^{15}N$ values of 3.13‰ at Maalaea could not occur as a result of mixing background groundwater with effluent.

The highest $\delta^{15}N$ value (4.6‰) at Maalaea could be a result of mixing effluent with background groundwater, but two component isotope mixing analysis suggests effluent is not present. Reported NO_3^- concentration of a near-coast irrigation well (well 4830-01; Dollar et al., 2011) is 190 μM. Salinity-unmixed NO_3^- concentration in the coastal groundwater sample with highest $\delta^{15}N$ (4.6‰) is 310 μM. Thus, we calculate the $\delta^{15}N$ of the 120 μM NO_3^- added to the groundwater system between the well and the coast as:

$$310 * \delta^{15}N_{sample} = 190 * \delta^{15}N_{BG} + 120 * \delta^{15}N_{added} \qquad (10)$$

where 310, 190, and 120 are the concentrations of the coastal sample, the well, and the added nitrate and $\delta^{15}N_{sample}$ = 4.6 ‰,, $\delta^{15}N_{BG}$ = 3.3‰ , and $\delta^{15}N_{added}$ is the value of the added nitrate. Solving, we find $\delta^{15}N_{added}$ is 7.0 ± 3.4 ‰, which is much lower than the values measured in effluent from the three Maui wastewater treatment facilities, which ranged from 14.7 – 31.5 ‰ (Hunt, 2007, Hunt and Rosa, 2009; Glenn et al., 2012). This suggests little injected wastewater is discharging to Maalaea coastal waters. The $\delta^{15}N$ of the 120 µM of added nitrate is at the higher end of values reported for fertilizers, though near the middle of the range of values reported for fertilized soils (Kendall, 1998). Thus, the high N+N concentrations observed at Maalaea are predominantly from fertilizers applied to the sugarcane, which overlies nearly the entire length of the groundwater flowpaths.

5.3.5 OSDS (Waiehu)

Waiehu has been identified as being at high risk from OSDS contamination to groundwater and coastal waters (Whittier and El-Kadi, 2014) and is the only field area other than Kahului that had elevated nitrate $\delta^{15}N$ values, which is suggestive of septic nitrate. Land use, groundwater flowpaths, wells, coastal samples, spring samples, $\delta^{15}N$ values, and NO_3^- concentrations for the area are detailed in Fig. 14A. Waiehu Bay is flanked by the Paukūkalo marsh, shown in Fig. 14A as a dark green sliver of undeveloped land. Coastal groundwater samples were collected along the beach on the seaward side of the marsh and two springs on the landward edge of the marsh. N+N concentrations measured in groundwater samples from the beach were low, ranging from below detection to 3.2 µM. By contrast the springs on the landward side of the marsh had N+N concentrations of 58.7 and 103.2 µM, respectively. Upslope wells varied in N+N concentration from 10.6 to 33.0 µM. Salinity unmixed $\delta^{18}O_{H20}$ values in Waiehu coastal samples were more negative than the values of some of the upslope wells, suggesting that the groundwater in the coastal samples was recharged at an elevation equal to or greater than the upslope wells. We suspect that the Paukūkalo marsh may act a coastal "nutrient filter" that reduces the flux of N to the coast (e.g. Fisher and Acreman, 2004; Nelson and Zavaleta, 2012), perhaps due to biological N uptake

by marsh plants, nitrate reduction within reducing marsh sediments, or other mechanisms. Whatever the mechanism, this apparently results in low observed nutrient concentrations in beachface and coastal water samples relative to spring samples collected from the landward edge of the marsh.

Using a two component isotope mass balance calculation we can determine if $\delta^{15}N$ value of nitrate in groundwater reflects an OSDS source. For this calculation we will ignore coastal samples as their chemistry appears to be affected by the marsh and assume well WW represents the upslope groundwater endmember. We also assume nitrate added to groundwater is the difference between that of the spring samples and well WW. Thus:

$$81.0 * \delta^{15}N_{sample} = 28.5 * \delta^{15}N_{WW} + 52.5 * \delta^{15}N_{added} \quad (11)$$

where 81.0, 28.5, and 52.5, are the mean coastal groundwater nitrate concentration, WW well nitrate concentration, and the concentration of the added nitrate, respectively. $\delta^{15}N_{sample}$ is the mean $\delta^{15}N$ value of the spring samples (12.7‰), $\delta^{15}N$ is the WW well value (1.7‰), and $\delta^{15}N_{added}$ is the value of the added nitrate. Solving, we find $\delta^{15}N_{added} = 18.7 \pm 4.4$‰ which is within the 10-20‰ range of values reported for OSDS nitrate. This mass balance suggests approximately 50 μM of OSDS derived nitrate is being added to groundwater in Waiehu on the landward side of the Paukūkalo marsh. But, because N+N concentrations in coastal samples are lower than the springs, it appears that much of the OSDS nitrate in groundwater measured at the springs is being lost prior to reaching the coast. Furthermore, the $\delta^{15}N$ values in the 2 of the 3 coastal samples are less than 5‰ which is not consistent with nitrate from an OSDS source. Although OSDS nitrate appears to be added to groundwater in Waiehu, the nutrients in that groundwater may be buffered by the marsh, resulting in low coastal water nutrient impact.

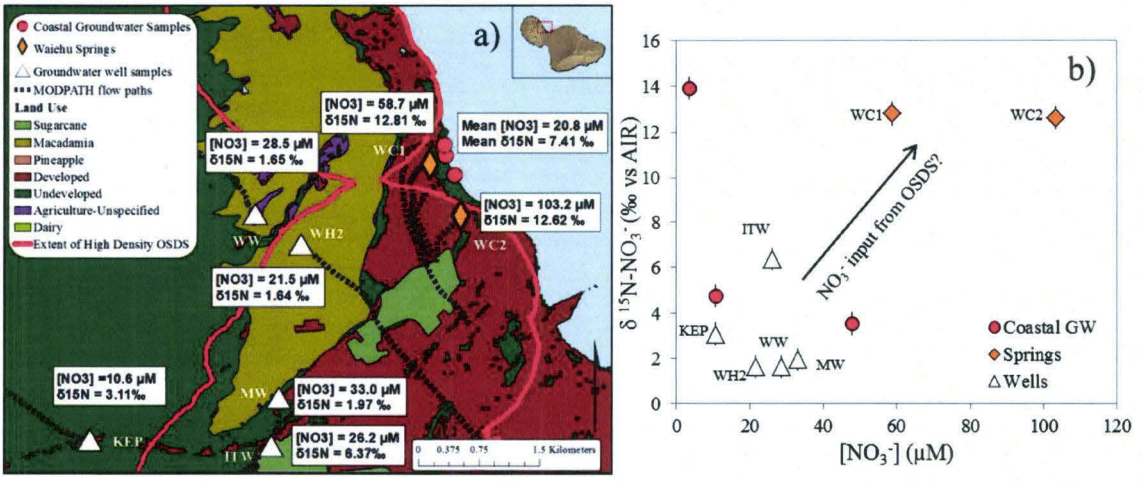

Fig. 14. Waiehu nutrient sources. a) Land use, groundwater flowpaths, wells, springs, coastal samples, δ15N values, and NO_3^- concentrations. b) binary plot of $\delta^{15}N$ vs NO_3^- concentration for Waiehu samples.

5.4 SGD Rates and Nutrient Fluxes

In Table 10 we present total and fresh SGD water and nutrient fluxes in order compare them to the fluxes measured in other studies in Maui and elsewhere in Hawaii. Our total fluxes were calculated by multiplying the scaled total SGD flux by the mean nutrient concentration measured in all coastal groundwater samples from a particular area. The difference between total and fresh SGD nutrient is small. This is because fresh SGD nutrient fluxes have relatively low water discharge with high nutrient concentrations, whereas total SGD nutrient fluxes have relatively high discharge and lower (more dilute) nutrient concentration. We believe that our rates are conservative as we assigned a minimum box size based on shore parallel radon surveys and the time series location. The width of the coastal box used in the model was defined by radon survey data collected at the time series location, which we believe provides a reasonable estimate of SGD plume width. The maximum seaward length of the box was defined by the time series location. Although the SGD plume extent may have reached further offshore than the time series location, we did not have the data required to determine the full extent of the plume and concluded a conservative estimate using the time series location is justified. Our SGD rates and nutrient fluxes presented here should be viewed as first order approximations because of the various

assumptions inherent in the application of radon box models (Burnett and Dulaiova 2003; Dulaiova et al. 2010; Swarzenski et al.2013) and because of uncertainties regarding seasonal variability.

Table 10. Comparison of SGD and associated nutrient fluxes in this study to past studies in the Hawaiian Islands. Because most previous work calculated nutrient fluxes for total SGD, we present total SGD nutrient fluxes in addition to fresh SGD nutrient fluxes.

Site	Fresh SGD ($m^3/m/d$)	Fresh PO_4^{3-} flux (mmoles/m/d)	Fresh Si flux (mmoles/m/d)	Fresh N+N flux (mmoles/m/d)
Kuau	3.8	19	3361	1666
Maalaea	4.1	30	2506	1192
Kahului	1.1	2.6	730	61
Honolua	4.4	8	2081	128
Waiehu	0.5	1.3	252	18
Honomanu	2.9	9.9	1974	23
Site and Study	**Total SGD ($m^3/m/d$)**	**Total PO_4^{3-} flux (mmoles/m/d)**	**Total Si flux (mmoles/m/d)**	**Total N+N flux (mmol/m/d)**
Kuau	4.4	19	3345	1660
Maalaea	11	50	4220	2072
Kahului	1.5	2.8	745	42
Honolua	5.9	9.1	2390	145
Waiehu	0.8	2.5	283	18
Honomanu	3.3	10	1952	21
Honolua, Maui[1]	2.5-21	1.2 - 8.7	-	6.2-72
Kahana, Maui[1*]	4.2 - 11	3.6 - 9.0	-	144 - 360
Kahana, Maui[1**]	250 - 530	200 - 430	-	8220 - 18000
Kahana, Maui[2]	35 - 113	-	-	1968
Mahinahina, Maui[1]	3.5 - 10	3 - 7.5	-	1840 - 6650
Honokowai, Maui[1]	2.7 - 7.2	0.5 - 9.0	-	54 - 153
Kahekili, Maui[3†]	21-55	90 - 1400	6980 - 32000	1400 - 4700
Kahekili, Maui[4†]	6 - 92	-	-	-
Hanalei, Kauai[5]	3.7 - 11	1.0 - 3.0	169 - 361	20 - 73
Haena, Kauai[5]	1.8 - 3.8	0.8 - 0.9	207 - 259	6.4 - 26
Kiholo, Hawaii[6]	34	150	24900	6400

*calculated using 1.56 day residence time

**calculated using 0.6 hr residence time

†fluxes were measured at springs discharging injected effluent and may be high due to the increased hydraulic gradient as a result of injection and high dissolved nutrient loads of the effluent.

[1]Street et al., 2008; [2]Paytan et al., 2006; [3] Swarzenski et al., 2012; [4]Glenn et al., 2012, 2013; [5]Knee et al., 2008; [6]Johnson, 2008b

Highest N+N fluxes calculated in this study occur at Kuau, where, based on N isotopic composition changes along a groundwater flowpath, we concluded that ~78% of coastal groundwater N+N is from fertilizers applied to commercial agriculture. As such, of the 1666 mmol/m/d of N+N that discharges to the coast at Kuau (Table 10), approximately 1300 mmol/m/d (78%) is from commercial agriculture and the remaining 366 mmol/m/d (22%) is from other sources. At Maalaea we estimate that, based on $\delta^{15}N$ values and the land use that groundwater flowpaths travel beneath, that nearly all of the approximately 1190 mmol/m/d of N+N discharging to coastal water via SGD is from fertilizers applied to sugarcane fields. At Honomanu, where groundwater flowpaths traveled beneath almost entirely undeveloped land, N+N flux was 23 mmol/m/d. Importantly, we find that the fertilizer-derived N+N fluxes at Kuau and Maalaea are more than 50 times higher than the N+N flux from the relatively pristine Honomanu areas, despite the fact that fresh discharge at Kuau and Maalaea are only 1.3 and 1.4 times higher than Honomanu, respectively. At Kahului, where wastewater is discharging to groundwater and coastal water, the nutrient flux is approximately 3 higher than at Honomanu, yet still 19 times less than the fertilizer derived flux from Kuau. These findings imply that land use, particularly commercial agriculture, can exert a substantial impact on local coastal SGD nutrient flux.

In order to compare our results to the nutrient fluxes of streams and rivers, we upscale the nutrient flux to the ocean for each field area by multiplying the fresh SGD nutrient flux per meter of shoreline by the length of shoreline transected by the radon survey (Table 11). We compare our fluxes to two west Maui ephemeral streams and also to the two largest rivers in the state, the Wailuku and Hanalei Rivers. Total dissolved nitrogen flux for the West Maui streams was between 78 and 390 moles/d (Soicher and Peterson, 1997). Thus, at Maalaea and Kuau, where the majority of N is from sugarcane and pineapple fields, the N flux to the ocean is as much as 62 times greater than those from the west Maui streams. The Hanalei River on north Kauai delivers 544,000 m^3/d of fresh water and an estimated 800 moles/d of N+N, 137 moles/d PO_4^{3-}, and 114,667 moles/d Si (Knee et al., 2008). The SGD N+N flux is 6 and 2 times greater at Kuau and Maalaea, respectively, than the N+N flux from the Hanalei River even though the

fresh SGD flux from these Maui sites are at most 5% of the Hanalei River discharge. SGD Si and PO_4^{3-} fluxes are lower than the Hanalei River fluxes, but still high for the amount of fresh SGD that discharges relative to riverine discharge. Wailuku River on east Hawai'i island delivers an estimated 170,000 m^3/d of fresh water during baseflow conditions and on average 660 moles/d of N+N, though during storms fresh discharge and nutrient flux can be 5-10 times higher (Weigner et al., 2009). Similarly, SGD at Kuau and Maalaea delivers N+N loads that are 8 and 3 times higher, respectively, than those delivered by the Wailuku River during baseflow conditions depite the fact that fresh SGD volumes are small (<7%) relative to the river discharge volume. Based on isotope mass balance, 3800 moles/d of N+N is discharging to the Kuau field area from fertilizers applied to commercial agriculture, or more than 4 times amount of N+N discharging to coastal waters from either of the two largest rivers in the State. It is apparent that SGD N+N fluxes in areas impacted by land use can be substantially larger the N fluxes from the state's two largest rivers, while SGD N+N fluxes from areas where land use has less impact are much smaller than riverine input.

Table 11. Upscaled SGD rates and nutrient fluxes. Below we present fresh SGD and associated nutrient fluxes at each field area after upscaling by the length of shoreline transected by the radon survey. River and stream discharge rates and nutrient fluxes are also shown.

Field Area	Length (m)	Upscaled Fresh Discharge (m^3/d)	PO_4^{3-} (moles/d)	Si (moles/d)	N+N (moles/d)
Kuau	2946	11200	55	9902	4909
Maalaea	1568	6430	46	3930	1869
Kahului	2754	3030	7	2011	167
Honolua	1061	4670	8	2209	135
Waiehu	1252	626	2	316	23
Honomanu	1043	3020	10	2059	24
Stream/River	**Island**	**Discharge (m^3/d)**	**PO_4^{3-} (mols/d)**	**Si (mols/d)**	**N+N (mols/d)**
Honokowai[1]	Maui	-	-	-	390*
Honokohua[1]	Maui	-	-	-	98
Hanalei[2]	Kaua'i	544000	140	114600	800
Wailuku[3]	Hawai'i	168000	-	-	660

* Total dissolved nitrogen was measured, not N+N
[1]Soicher and Peterson, 1997; [2]Knee et al., 2008; [3]Weigner et al., 2009

6. Conclusions

In this study we employed a combined methodology to determine the source, transport, and rate of nutrients to the ocean via submarine groundwater discharge by combining numerical groundwater modeling, geochemical mass balance modeling, and stable isotope biogeochemistry. By combining groundwater and geochemical modeling with stable isotope analysis we were able to successfully connect land use practices along groundwater flowpaths with the nutrient fluxes to the ocean at the end of those flowpaths. Multiple regression and $\delta^{15}N$ values both suggest that commercial agriculture, particularly sugarcane, contributes the greatest amount of N+N to the ocean via SGD. Groundwater travel times in Hawai'i occur on decadal time scales (Kelly et al., 2015), thus the N+N from sugarcane and pineapple measured during this study likely represent both present and past contributions. Because sugarcane and, to a lesser extent pineapple, persists on Maui and because groundwater travel times on Maui are slow, the N+N flux from these agricultural practices will likely continue, even after production stops.

Our analysis of the Waiehu, Kuau, and Maalaea areas, where there is moderate to high risk of OSDS contamination to groundwater (Whittier and El-Kadi, 2014), or small scale wastewater injection, showed mixed results in terms of identifying OSDS or wastewater derived nitrate. This may be because OSDS or wastewater nitrate is not present in groundwater near Kuau or Maalaea or that $\delta^{15}N$ values are not always sufficient in identifying OSDS or wastewater nitrate. $\delta^{15}N$ values could be used to identify OSDS nitrate in groundwater near Waiehu where there is high OSDS risk, though the amount of N+N was relatively small. Similarly, $\delta^{15}N$ values suggest effluent discharges to groundwater and coastal water near Kahului where large volumes of wastewater are injected, but N+N fluxes and concentrations at Kahului are fairly low. Although N+N contributions from OSDS and wastewater appear to be low at these locations, the presence of OSDS and effluent is of concern because these waste sources may contribute bacteria, heavy metals, pharmaceuticals or other contaminants to groundwater and coastal water (Al-Bahry et al., 2014).

This work demonstrates that even though SGD water volume fluxes are much smaller, the coastal SGD N fluxes delivered from areas impacted by land use can be substantially larger than the N fluxes delivered from that of the State of Hawaii's two largest rivers. The large variation in N+N fluxes among the field areas studied is primarily a result of the differences in groundwater endmember N+N concentration; whereas fresh water SGD flux varied by a factor of only 8 between areas with the lowest and highest discharge, the fresh water N+N concentration and resultant N+N flux varied by a factors of 55 and 92, respectively. At areas such as Kuau and Maalaea where there was a high fresh SGD flux and high groundwater nutrient endmember nutrient concentration, the risk of nutrient pollution by SGD is substantial. Thus, both groundwater endmember nutrient concentrations and fresh SGD flux must be considered when assessing coastal water nutrient pollution vulnerability in Hawai'i.

References

Al-Bahry, S.N., Mahmoud I.Y., Paulson, J.R., and Al-Musharafi, S.K., 2014. Survival and growth of antibiotic resistant bacteria in treated wastewater and water distribution system and their implication in human health: A review. The International Arabic Journal of Antimicrobial Agents, v. 4, p. 1-11. DOI: 10.3823/758.

Berry, W.D., and Feldman, S., 1985. Multiple Regression in Practice. Sage University Paper, series on Quantitative Applications in the Social Science, 07-050. London.

Böhlke, J.-K., 2003. Sources, transport, and reaction of nitrate. In: Lindsey, B.D., and Phillips, S.W., Donnelly, C.A., Speiran, G.K., Plummer, L.N., Böhlke, J.-K., Focazio, M.J., Burton, W.C., and Busenberg, E., Residence times and nitrate transport in ground water discharging to streams in the Chesapeake Bay Watershed: U.S. Geological Survey Water-Resources Investigations Report 03-4035, p. 25-39. http://pa.water.usgs.gov/reports/wrir03-4035.pdf.

Borah, D.K., and Bera, M., 2004. Watershed-scale hydrologic and nonpoint-source pollution models: Review of applications. American Society of Agricultural Engineers, v. 47, p. 789-803. DOI: 10.13031/2013.16110.

Burnett, W.C. and Dulaiova, H., 2003. Estimating the dynamics of groundwater input into the coastal zone via continuous radon-222 measurements. Journal of Environmental Radioactivity, v. 69, p. 21-35. DOI:10.1016/S0265-931X(03)00084-5.

Burnham, W.L., Larson,S.P., Cooper, H.H.J., 1977. Distribution of injected wastewater in the saline lava aquifer, Wailuku-Kahului wastewater treatment facility, Kahului, Maui, Hawaii. Open-file Report 77-469. http://pubs.er.usgs.gov/publication/ofr77469.

Casciotti, K.L., Sigman, D.M., Hastings, M.G., Bohlke, J.K., and Hilkert, A., 2002. Measurement of the oxygen isotopic composition of nitrate in seawater and freshwater using the denitrifier method. Analytical Chemistry, v. 74, p. 4908-4912. DOI: 10.1021/ac020113w.

Cesar, S.F., and van Beukering, P. J. H.. 2004. Economic valuation of the coral reefs of Hawai'i. Pac. Sci. v. 58, p. 231-242. http://scholarspace.manoa.hawaii.edu/bitstream/handle/10125/2723/vol58n2-231-242.pdf?sequence=1.

County of Maui, Department of Public Works, 1990. Environmental Assessment and Negative Declaration for the Wailuku-Kahului Wastewater Reclamation facilities Additions and Modifications. http://oeqc.doh.hawaii.gov/Shared%20Documents/EA_and_EIS_Online_Library/Maui/1990s/1990-12-08-MA-FEA-WAILUKU-KAHULUI-WASTEWATER-RECLAMATION.pdf

Dailer, M.L., Knox, R.S., Smith, J.E., Napier, M., Smith,C., 2010. Using $\delta^{15}N$ values in algal tissue to map locations and potential sources of anthropogenic nutrient inputs on the island of Maui, Hawaii, USA. Marine Pollution Bulletin, v. 60, p. 655-671. DOI:10.1016/j.marpolbul.2009.12.021. http://coralreefecology.ucsd.edu/files/2010/09/Dailer_et-al_2010_MPB.pdf.

Dailer, M.L., Smith, J.E., and Smith, C.M., 2012. Responses of bloom forming and non-bloom forming macroalgae to nutrient enrichment in Hawai'i, USA, Harmful Algae, v. 17, p. 111-125. http://dx.doi.org/10.1016/j.hal.2012.03.008.

Dollar, S. and Andrews, C., 1997. Algal blooms off west Maui: Assessing causal linkages between land and the coast ocean. University of Hawaii at Manoa, Final Report, 40 p.

Dollar, S., Atkinson, M., Hochberg, E., and Nance, T., 2011. An Evaluation of Causal Factors Affecting Coral Reef Community and Benthic Structure in Maalaea Bay, Maui, Hawaii. Final Report of the Maalaea Bay Coral Reef Degradation Study prepared for the county of Maui, 84 p. http://hi-mauicounty.civicplus.com/DocumentCenter/View/83262.

Dulaiova. H., Peterson. R., Burnett, W.C., and Lane-Smith, D., 2005. A multi-detector continuous monitor for assessment of 222Rn in the coastal ocean. Journal of Radioanalytical and Nuclear Chemistry, v. 263, p. 361-365. DOI: 10.1007/s10967-005-0063-8.

Dulaiova, H., Camilli, R., Henderson, P.B., Charette, M.A., 2010. Coupled radon, methane and nitrate sensors for large-scale assessment of groundwater discharge and non-point source pollution to coastal waters. Journal of Environmental Radioactivity v. 101, p. 553-563. DOI:10.1016/j.jenvrad.2009.12.004

Engott, J.A and Vana, T.T., 2007. Effects of agricultural land-use changes and rainfall on groundwater recharge in central and west Maui, Hawaii, 1926-2004. USGS Scientific Investigation Report, 2007-5103. http://pubs.usgs.gov/sir/2007/5103/sir2007-5103.pdf.

Falconer, J.K., 1991. Sugarcane Fertilization Practices on the Island of Maui. Proceedings of the 50th annual conference of Sugarcane Technologists, Honolulu, HI, November 11-13, 1991, p A-22 - A-24.

Fisher, J., and Acreman, M.C., 2004. Wetland nutrient removal: a review of evidence. Hydrology and Earth System Science, v. 8, p. 673 – 685. http://www.hydrol-earth-syst-sci.net/8/673/2004/hess-8-673-2004.pdf

Giambelluca, T.W., Chen, Q., Frazier, A.G., Price, J.P., Chen, Y.-L., Chu, P.-S., Eischeid, J.K., Delparte, D.M., 2011. The Rainfall Atlas of Hawai'i 2011- Final Report. http://rainfall.geography.hawaii.edu

Giambelluca, T.W., Chen, Q., Frazier, A.G., Price, J.P., Chen, Y.-L., Chu, P.-S., Eischeid, J.K., Delparte, D.M., 2013. Online rainfall atlas of Hawai'i. Bulletin of the American Meteorilogical Society, v. 94, p. 313-316. DOI: 10.1175/BAMS-D-11-00228.1.

Gingerich, S.B., 2008. Ground-water availability in the Wailuku area, Maui, Hawai'i. USGS Scientific Investigations Report 2008-5236.

Glenn, C.R., Whittier, R.B., Dailer, M.L., Dulaiova, H., El-Kadi, A.I., Fackrell, J., Kelly, J.L., and Waters, C.A., 2012, 2013. Lahaina Groundwater Tracer Study – Lahaina, Maui, Hawai'i. Final Interim Report. Prepared from the State of Hawai'i Department of Health, the U.S. Environmental Protection Agency, and the U.S. Army Engineer Research and Development Center, 463p. http://www.epa.gov/region9/water/groundwater/uic-pdfs/lahaina02/lahaina-final-interim-report.pdf.

Glenn, C.R., Whittier, R.B., Dailer, M.L., Dulaiova, H., El-Kadi, A.I., Fackrell, J., Kelly, J.L.. Waters, C.A. and Sevadjian, J., 2013. Lahaina groundwater tracer study—Lahaina, Maui, Hawai'i, Final Report. Prepared from the State of Hawai'i Department of Health, the U.S. Environmental Protection Agency, and the U.S. Army Engineer Research and Development Center. 502p. http://www.epa.gov/region9/water/groundwater/uic-pdfs/lahaina02/lahaina-gw-tracer-study-final-report-june-2013.pdf.

Granger, J., Sigman, D.M., Prokopenko, M.G., Lehmann, M.F., and Tortell, P.D., 2006. A method for nitrite removal in nitrate N and O isotope analyses. Limnology and Oceanography: Methods, v. 4, p. 205-212.

Harbaugh, A.W., 2005. MODFLOW-2005, The U.S. Geological Survey modular ground-water model – the ground-water flow process. U.S. Geological Survey Techniques and Methods 6-A16. http://pubs.usgs.gov/tm/2005/tm6A16/.

Herzfeld, I. 2011. Physical regulation of land-ocean CNP flux and relationships to macroalgae blooms across coastal zones of Maui. Ph.D. Dissertation from the Department of Oceanography, Honolulu Hawaii: University of Hawaii at Manoa, 252p.

Houlton, B.Z., Sigman, D.M., and Hedin, L.O., 2006. Isotopic evidence for large gaseous nitrogen losses from tropical rainforests. Proceedings from the National Academy of Sciences, v. 103, p. 8745-8750. http://www.ncbi.nlm.nih.gov/pubmed/16728510.

Hunt, C.D., Jr., 2007. Ground-water nutrient flux to coastal waters and numerical simulation of wastewater injection at Kihei, Maui, Hawaii: U.S. Geological Survey Scientific Investigations Report 2006-5283, 69p. http://pubs.usgs.gov/sir/2006/5283/.

Hunt, C.D. and Rosa S.N., 2009. A multitracer approach to detecting wastewater plumes at Kihei and Lahaina, Maui, Hawaii. USGS Scientific Investigations Report 2009–5253, 166p. http://pubs.usgs.gov/sir/2009/5253/.

Johnson, A.G., 2008. Groundwater Discharge from the Leeward Half of the Big Island of Hawaii. M.S. Thesis from the Department of Geology and Geophysics, Honolulu Hawaii: University of Hawaii at Manoa, 145p.

Johnson, A.G., Glenn, C.R., Burnett, W.C., Peterson, R.N., and Lucey, P.G., 2008. Aerial infrared imaging reveals large nutrient-rich groundwater inputs to the ocean. Geophysical Research Letters, v. 35. doi: 10.1029/2008GL034574.

Kaushal, S.S., Grosman, P.M., Band, L.E., Elliott, E.M., Shields, C.A., and Kendall, C., 2011. Tracking nonpoint source nitrogen pollution in human-impacted watersheds. Environmental Science and Technology, v. 45, p. 8225-8232. DOI: 10.1021/es200779e. http://pubs.acs.org/doi/ipdf/10.1021/es200779e.

Keith, T.Z., 2006. Multiple Regression and Beyond, 2nd Edition. Boston, MA, Pearson Education, 534 p.

Kelly, J.K. 2012. Identification and quantification of submarine groundwater discharge in the Hawaiian Islands. Ph.D. Dissertation from the Department of Geology and Geophysics, 811p, Honolulu Hawaii: University of Hawaii at Manoa.

Kelly, J.L., Glenn, C. R., 2015. Chlorofluorocarbon apparent ages of groundwaters from west Hawaii, USA. Journal of Hydrology. DOI:10.1016/j.jhydrol.2015.04.069. http://dx.doi.org/10/1016/j.hydrol.2015.04.069.

Kendall, C., 1998. Tracing Nitrogen Sources and Cycling in Catchments, *in* Kendall, C., and McDonnell, J.J., eds., Isotope Tracers in Catchment Hydrology: Amsterdam, Elsevier, p. 519-576. http://wwwrcamnl.wr.usgs.gov/isoig/isopubs/itchch16.html.

Knee, K.L., Layton, B., Street, J.H., Boehm, A., Paytan, A., 2008. Sources of nutrients and fecal indicator bacteria to nearshore waters on the north shore of Kauai (Hawaii, USA). Estuaries and Coasts, DOI 10.1007/s12237-008-9055-6.

Knee, K.L., Street, J.H., Grossman, E.E., Boehm, A.B., Paytan, A., 2010. Nutrient inputs to the coastal ocean from submarine groundwater discharge in a groundwater-dominated system: Relation to land use (Kona coast, Hawaii, U.S.A.). Limnology and Oceonography, v. 55, p. 1105-1122. DOI:10.4319/lo.2010.55.3.1105.

Lapworth, D.J., Gooddy, D.C., Kent, F., Heaton, T.H.E., Cole, S.J., Allen, D, 2013. A combined geochemical and hydrological approach for understanding macronutrient sources. Journal of Hydrology, v. 500, p. 226-242. DOI:10.1016/j.jhydrol.2013.07.006.

Laws, E., Brown, D., Peace, C., 2004. Coastal water quality in the Kihei and Lahaina districts of the island of Maui, Hawaiian Islands. Impacts from physical habitat and groundwater seepage:

Implications for water quality standards. International Journal of Environment and Pollution, v. 22, p. 531-546.

McIlvin, M.R., and Casciotti, K.L., 2011. Technical Updates to the bacterial method for nitrate isotopic analyses. Analytical Chemistry, v. 84, p. 1850-1856. DOI: 10.1021/ac1028984

McMahon, P.B. and Bohlke, J.K. 2006. Regional Patterns in the isotopic composition of natural and anthropogenic nitrate in groundwater, High Plains, U.S.A. Environmental Science and Technology, v. 40, p. 2965-2970. DOI: 10.1021/es052229q.

Nelson, J.L., and Zavaleta, E.S., 2012. Salt marhs as a coastal filter for oceans:Changes in function with experimental increases in nitrogen loading and sea-level rise. PLoS ONE, v. 7, e38558. doi:10.1371/journal.pone.0038558.

NOAA, 2012. National Oceanic and Atmospheric Administration (NOAA). Coastal Change Analysis Program Regional Land Cover (C-CAP) Hawaii 2005 Land Cover. NOAA Ocean Service, Office for Coastal Management. http://coast.noaa.gov/digitalcoast/data/ccapregional

NOAA, 2007. National Oceanic and Atmospheric Administration (NOAA). Digital elevation models for the main 8 Hawaiian islands. National Ocean Service, National Center's for Coastal ocean Science, Silver Springs, MD. http://ccma.nos.noaa.gov/products/biogeography/mapping/dems/

Paytan, A., Shellenberger, G.G., Street, J.H., Gonneea, M., Davis, K., Young, M.B., and Moore, W.S., 2006. Submarine groundwater discharge: An important source of new inorganic nitrogen to coral reef ecosystems. Limnology and Oceanography 51: 343-348. DOI: 10.4319/lo.2006.51.1.0343.

Pollock, D.W., 2012. User guide for MODPATH version 6 – A particle-tracking model for MODFLOW. U.S. Geological Survey Techniques and Methods 6-A41, 58 p. http://pubs.usgs.gov/tm/6a41/.

Scholl, M.A., Gingerich, S.B., and Tribble, G.W., 2002. The influence of microclimates and fog on stable isotope signatures used in interpretation of regional hydrology, East Maui, Hawaii: Journal of Hydrology, v. 264, p. 170-184. DOI: 10.1016/S0022-1694(02)00073-2.

Scholl, M.A., Ingebritsen, S.E., Janik, C.J., and Kauahikaua, J.P., 1996. Use of precipitation and groundwater isotopes to interpret regional hydrology on a tropical volcanic island: Kilauea volcano area, Hawaii: Water Resources Research, v. 32, p. 3525-3537. DOI: 10.1029/95WR02837.

Singleton, M.J., Woods, K.N., Conrad, M.E., DePaolo, D.J., and Dresel, P.E. 2005. Tracking sources of unsaturated zone and groundwater nitrate contamination using nitrogen and oxygen stable isotopes at the Hanford Site, Washington. Environmental Science and Technology, v. 39, p. 3563-3570. DOI: 10.1021/es0481070

Sigman, D.M., Casciotti, K.L., Andreani, M., Barford, C., Galanter, M., and Bohlke, J.K., 2001. A bacterial method for the nitrogen isotopic analysis of nitrate in seawater and freshwater. Analytical Chemistry, v. 73, p. 4145-4153. DOI: 10.1021/ac010088e

Soicher, A.J. and Peterson, F.L., 1997. Terrestrial nutrient and sediment fluxes to the coastal waters of West Maui, Hawaii. Pacific Science, v. 51, p. 221-232. http://scholarspace.manoa.hawaii.edu/bitstream/handle/10125/3143/v51n3-221-232.pdf?sequence=1.

State of Hawaii, 2008. Water Resource Protection Plan, June 2008: Commission on Water Resource Management, 556 p.

Stearns, H.T., Macdonald, G.A., 1942. Geology and groundwater resources of the island of Maui, Hawaii. U.S. Geological Survey Bulletin 7.

Street, J.H., Knee, K. L., Grossman, E.E., and Paytan, A., 2008. Submarine groundwater discharge and nutrient addition to the coastal zone and coral reefs of leeward Hawaii. Marine Chemistry, v. 109, p. 355-376. DOI: 10.1016/j.marchem.2007.08.009.

Swarzenski, P.W., Storlazzi, C.D., Presto, M.K., Gibbs, A.E., Smith, C.G., Dimova, N.T., Dailer, M.L., and Logan, J.B., 2012. Nearshore morphology, benthic structure, hydrodynamics, and coastal groundwater discharge near Kahekili Beach Park, Maui, Hawaii. U.S. Geological Survey Open File Report 2012-1166. http://pubs.usgs.gov/of/2012/1166/.

Swarzenski, P.W., Dulaiova, H., Dailer, M.L., Glenn, C.R., Smith, C.G., Storlazzi, C.D., 2013. A geochemical and geophysical assessment of coastal groundwater discharge at select sites in Maui and O'ahu, Hawai'i. In *Groundwater in the Coastal Zones of Asia-Pacific*, p 27-46. Springer Netherlands.

van Beukering, P. J. H., and H. S. J. Cesar. 2004. Ecological economic modeling of coral reefs: Evaluating tourist overuse at Hanauma Bay and algae blooms at the Kihei coast, Hawai'i. Pacific Science, v. 58, p. 243- 260. DOI: 10.1353/psc.2004.0012.

Wankel, S.D., Kendall, K., Francis, C.A., and Paytan, A., 2006. Nitrogen sources and cycling in the San Francisco Bay Estuary: A nitrate dual isotopic composition approach. Limnology and Oceanography, vol. 51, p. 1654-1664. DOI: 10.4319/lo.2006.51.4.1654.

Weigner, T.N., Tubal, R.L., MacKenzie, R.A., 2009. Bioavailability and export of dissolved organic matter from a tropical river during base and stormflow conditions. Limnology and Oceanography, v. 54, p. 1233-1242. DOI: 10.4319/lo.2009.54.4.1233. http://www.aslo.org/lo/toc/vol_54/issue_4/1233.pdf.

Whittier, R. B., Rotzoll, K., Dhal, S., El-Kadi, A. I., Ray, C., Chang, D., 2010. Groundwater source assessment program for the state of Hawaii, USA: methodology and example

application. Hydrogeology Journal, v. 18, p. 711-723. DOI: 10.1007/s10040-009-0548-6. http://link.springer.com/article/10.1007%2Fs10040-009-0548-6.

Whittier, R. B. and El-Kadi, A. I., 2014. Human Health and Environmental Risk Ranking of Onsite Sewage Disposal Systems for the Hawaiian Islands of Kauai, Maui, Molokai, and Hawaii. Report submitted, State of Hawaii Department of Health and Safe Drinking Water Branch, Honolulu, HI, 258 pp.

Yates, M.V., 1985. Septic tank density and groundwater contamination. Groundwater vol. 23, p. 586-591. DOI: 10.1111/j.1745-6584.1985.tb01506.x.

Young, C., Tamborski, J., Bokuniewicz, H., 2015. Embayment scale assessment of submarine groundwater discharge nutrient loading an associated land use. Estuarine, Coastal, and Shelf Science, v. 158, p. 20-30. DOI:10.1016/j.ecss.2015.02.006. http://www.sciencedirect.com/science/article/pii/S0272771415000530#.

Appendix

A 1. Water samples. Water sample type, field area where the sample was collected, collection date. latitude (lat)., longitude (lon), salinity, and dissolved oxygen percent saturation.

Sample Name	Sample Type	Field Location	Date	Lat	Lon	Salinity	DO %
WC1	Spring	Waiehu	3/27/2014	20.91445	-156.49365	1.00	40.8
WC2	Spring	Waiehu	3/27/2014	20.90850	-156.49000	0.47	92.6
IST	Stream	Waiehu	3/27/2014	20.90950	-156.48535	0.05	115.1
WM1	Marine	Waiehu	3/28/2014	20.91640	-156.49170	30.78	85.4
WM2	Marine	Waiehu	3/28/2014	20.91720	-156.49180	20.70	100.8
WM3	Marine	Waiehu	3/28/2014	20.91683	-156.49080	35.35	105.5
WP1	Piezometer	Waiehi	3/28/2014	20.91657	-156.49190	9.20	42.5
WP2	Piezometer	Waiehu	3/28/2014	20.91708	-156.49190	1.73	22.3
WB-ST	Stream	Waiehu	7/21/2013	20.91791	-156.49174	0.04	-
WB-SP1	Spring	Waiehu	7/21/2013	20.91712	-156.49191	2.58	-
WBP-1	Piezometer	Waiehu	7/21/2013	20.91534	-156.49173	24.89	-
WBP-2	Piezometer	Waiehu	7/21/2013	20.91317	-156.49069	32.49	-
WBP-3	Piezometer	Waiehu	7/24/2013	20.91041	-156.48582	18.98	22.2
WBA-23	Marine	Waiehu	7/22/2013	20.91673	-156.49157	28.81	136.9
WBA-24	Marine	Waiehu	7/22/2013	20.91680	-156.49137	29.89	106.8
WBA-25	Marine	Waiehu	7/22/2013	20.91690	-156.49105	34.57	104.3
WBA-26	Marine	Waiehu	7/22/2013	20.91757	-156.49003	34.70	94.8
WBA-27	Marine	Waiehu	7/22/2013	20.91623	-156.49167	29.65	134.9
WBA-28	Marine	Waiehu	7/22/2013	20.91553	-156.49152	30.49	120.1
WBA-29	Marine	Waiehu	7/22/2013	20.91478	-156.49120	32.46	106.1
WBA-30	Marine	Waiehu	7/22/2013	20.91293	-156.49038	32.87	93.1
WBA-31	Marine	Waiehu	7/22/2013	20.91048	-156.48790	33.61	96.8
WBA-32	Marine	Waiehu	7/22/2013	20.91110	-156.48633	34.51	100.3
-	-	-	-	-	-	-	-
KWP-9	Piezometer	Kahului	3/29/2014	20.89643	-156.45354	19.01	61.4
KWM-TS	Marine	Kahului	3/29/2014	20.89689	-156.45464	32.83	90.2
KWM-2	Marine	Kahului	3/29/2014	20.89793	-156.45436	34.12	92.6
KWM-3	Marine	Kahului	3/29/2014	20.89931	-156.45436	34.59	101.7
KWB-1	Marine	Kahului	7/24/2013	20.89741	-156.45981	32.01	77.8
KWB-2	Marine	Kahului	7/24/2013	20.89713	-156.45714	30.24	89.2
KWB-3	Marine	Kahului	7/24/2013	20.89650	-156.45364	32.48	104.8
KWB-4	Marine	Kahului	7/24/2013	20.89662	-156.45110	32.55	103.1
KWP-1	Piezometer	Kahului	7/19/2013	20.90063	-156.44052	1.58	-
KWP-2	Piezometer	Kahului	7/19/2013	20.89970	-156.44278	10.68	-
KWP-3	Piezometer	Kahului	7/19/2013	20.89895	-156.44670	7.49	-
KWP-4	Piezometer	Kahului	7/20/2013	20.89686	-156.45566	9.37	-
KWP-5	Piezometer	Kahului	7/20/2013	20.89732	-156.46002	7.83	-

Sample Name	Sample Type	Field Location	Date	Lat	Lon	Salinity	DO %
KWP-6	Piezometer	Kahului	7/20/2013	20.89648	-156.45349	6.75	-
KWP-7	Piezometer	Kahului	7/20/2013	20.89656	-156.45174	8.95	-
KWP-8	Piezometer	Kahului	7/20/2013	20.89695	-156.44879	2.16	-
KWA-X1	Marine	Kahului	7/23/2013	20.90052	-156.44295	33.22	93.2
KWA-TS	Marine	Kahului	7/23/2013	20.89699	-156.45493	31.58	85
KWA-14	Marine	Kahului	7/23/2013	20.90288	-156.45728	34.66	89.4
KWA-17	Marine	Kahului	7/23/2013	20.89845	-156.46176	34.29	89.6
KWA-18	Marine	Kahului	7/23/2013	20.89860	-156.46455	34.19	93.4
KWA-19	Marine	Kahului	7/23/2013	20.90141	-156.46483	34.61	104.8
KWA-20	Marine	Kahului	7/23/2013	20.90505	-156.46538	34.88	106.1
KWA-21	Marine	Kahului	7/23/2013	20.90552	-156.45685	34.65	96.5
KWA-23	Marine	Kahului	7/23/2013	20.90092	-156.45730	34.43	91.2
KWA-24	Marine	Kahului	7/23/2013	20.89945	-156.45715	34.14	104
KWA-25	Marine	Kahului	7/23/2013	20.89847	-156.45924	34.00	74.2
KWA-26	Marine	Kahului	7/23/2013	20.89855	-156.45712	33.96	108.9
KWA-27	Marine	Kahului	7/23/2013	20.89827	-156.45457	33.35	79.2
KWA-28	Marine	Kahului	7/23/2013	20.89826	-156.45160	33.21	70.4
KWA-29	Marine	Kahului	7/23/2013	20.90474	-156.44746	33.90	54.7
KWA-30	Marine	Kahului	7/23/2013	20.90159	-156.44748	33.82	69.2
KWA-31	Marine	Kahului	7/23/2013	20.89939	-156.44702	33.60	69.4
KWA-32	Marine	Kahului	7/23/2013	20.90085	-156.44133	30.03	71.7
Kan	Pond	Kahului	7/23/2013	20.89471	-156.45825	27.28	132.8
KWWTP	Effluent	Kahului	7/23/2013	20.89699	-156.45493	4.90	76.1
-	-	-	-	-	-	-	-
MP1	Piezometer	Maalaea	3/30/2014	20.79213	-156.50970	1.22	87.2
MP2	Piezometer	Maalaea	3/30/2014	20.79242	-156.51003	7.29	74.8
MP3	Piezometer	Maalaea	3/30/2014	20.79235	-156.50949	1.53	84.6
MP4	Piezometer	Maalaea	3/30/2014	20.79337	-156.50848	4.26	82.6
MP5	Piezometer	Maalaea	3/30/2014	20.79514	-156.50633	34.59	101.8
MM-1	Marine	Maalaea	3/30/2014	20.79000	-156.50909	35.80	116.9
MM-2	Marine	Maalaea	3/30/2014	20.79130	-156.50929	34.35	147.6
MM3	Marine	Maalaea	3/30/2014	20.79175	-156.50945	34.52	146.5
MM4	Marine	Maalaea	3/30/2014	20.79342	-156.50140	35.83	109.1
MM5	Marine	Maalaea	3/30/2014	20.79393	-156.50116	35.85	109
MM6	Marine	Maalaea	3/30/2014	20.79483	-156.50124	35.83	110.5
MM7	Marine	Maalaea	3/30/2014	20.79603	-156.50156	35.61	105
MM8	Marine	Maalaea	3/31/2014	20.79221	-156.50957	30.18	125.3
MM9	Marine	Maalaea	3/31/2014	20.79467	-156.50685	29.89	124
MM10	Marine	Maalaea	3/31/2014	20.79430	-156.50660	33.73	122.2
MM11	Marine	Maalaea	3/31/2014	20.79363	-156.50612	35.74	108.6

Sample Name	Sample Type	Field Location	Date	Lat	Lon	Salinity	DO %
MM12	Marine	Maalaea	3/31/2014	20.79570	-156.50150	35.64	125.8
MBP-1	Piezometer	Maalaea	7/30/2012	20.79231	-156.50977	25.61	88.9
MBP-1A	Piezometer	Maalaea	7/31/2012	20.79231	-156.50977	20.72	34.1
MBP-2	Piezometer	Maalaea	7/30/2012	20.79238	-156.50960	32.92	99
MBP-3	Piezometer	Maalaea	8/1/2012	20.79507	-156.48534	34.74	60.9
MBP-4	Piezometer	Maalaea	8/1/2012	20.79658	-156.50317	34.00	95.8
MBP-5	Piezometer	Maalaea	8/1/2012	20.78991	-156.51402	34.23	97.2
MBP-6	Piezometer	Maalaea	8/1/2012	20.77606	-156.52925	35.06	95.3
MBA-1	Marine	Maalaea	7/31/2012	20.79197	-156.50970	31.00	93.4
MBA-2	Marine	Maalaea	7/31/2012	20.79148	-156.50972	33.30	92.2
MBA-3	Marine	Maalaea	7/31/2012	20.79085	-156.50974	34.48	97.2
MBB-1	Marine	Maalaea	8/3/2012	20.79220	-156.50960	28.80	-
MBB-2	Marine	Maalaea	8/3/2012	20.79203	-156.50948	33.00	-
MBB-3	Marine	Maalaea	8/3/2012	20.79133	-156.50947	33.60	-
MBB-4	Marine	Maalaea	8/3/2012	20.79037	-156.50935	33.50	-
MBC-1	Marine	Maalaea	8/3/2012	20.79278	-156.50860	28.51	-
MBC-2	Marine	Maalaea	8/3/2012	20.79245	-156.50845	31.90	-
MBC-3	Marine	Maalaea	8/3/2012	20.79175	-156.50810	33.80	-
-	-	-	-	-	-	-	-
HP1	Piezometer	Honolua	4/1/2014	21.01404	-156.63776	0.92	82.8
HP2	Piezometer	Honolua	4/1/2014	21.01320	-156.63902	0.65	98.7
HP3	Piezometer	Honolua	4/1/2014	21.01326	-156.63942	8.89	101.3
HBSP1	Coastal Spring	Honolua	4/1/2014	21.01324	-156.63969	13.07	94.3
HBSP2	Coastal Spring	Honolua	4/1/2014	21.01326	-156.63998	1.02	102.5
HBSP3	Coastal Spring	Honolua	4/1/2014	21.01342	-156.64070	3.47	103.4
HBTS	Marine	Honolua	4/1/2014	21.01325	-156.63942	30.26	105.2
HBM-1	Marine	Honolua	4/1/2014	21.00482	-156.38221	31.62	106.5
HBM-2	Marine	Honolua	4/1/2014	21.01355	-156.63970	34.66	117.6
HBM-3	Marine	Honolua	4/1/2014	21.01384	-156.64000	35.02	116.6
HBM-4	Marine	Honolua	4/1/2014	21.01436	-156.64070	33.94	107.7
HBST	Stream	Honolua	4/1/2014	21.01299	-156.63722	0.02	102.8
HBA-1	Marine	Honolua	8/2/2012	21.01333	-156.63944	33.20	99.7
HBA-1-5	Marine	Honolua	8/2/2012	21.01345	-156.63950	34.12	98.6
HBA-2	Marine	Honolua	8/2/2012	21.01353	-156.63952	34.22	98.4
HBA-3	Marine	Honolua	8/2/2012	21.01366	-156.63958	34.17	98.8
HBA-3-5	Marine	Honolua	8/2/2012	21.01375	-156.63962	34.06	100.1
HBA-4	Marine	Honolua	8/2/2012	21.01385	-156.63973	34.04	101.6
HBA-5	Marine	Honolua	8/2/2012	21.01407	-156.63971	34.04	98.9
HBA-6	Marine	Honolua	8/2/2012	21.01432	-156.64005	34.40	97.1
HBM-1	Marine	Honolua	8/2/2012	21.01328	-156.63887	31.30	123.4

Sample Name	Sample Type	Field Location	Date	Lat	Lon	Salinity	DO %
HBTS-1	Marine	Honolua	7/29/2012	21.01339	-156.63960	33.30	
HBSP-A	Coastal Spring	Honolua	8/2/2012	21.01325	-156.63997	0.40	110.6
HBSP-B	Coastal Spring	Honolua	8/2/2012	21.01319	-156.63983	1.30	110.6
HBSP-C	Coastal Spring	Honolua	8/2/2012	21.01319	-156.63907	19.50	102
-	-	-	-	-	-	-	-
HMP-1	Piezometer	Honomanu	4/3/2014	20.86052	-156.16563	8.18	91.9
HMSP1	Piezometer	Honomanu	4/3/2014	20.86054	-156.16536	4.61	71.3
HMM1	Marine	Honomanu	4/3/2014	20.86058	-156.16646	10.64	106.1
HMM2	Marine	Honomanu	4/3/2014	20.86261	-156.16682	34.12	106.4
HMST	Stream	Honomanu	4/3/2014	20.86078	-156.16690	0.04	106.1
HMP-1	Piezometer	Honomanu	7/9/2013	20.86055	-156.16568	0.90	-
HMP-2	Piezometer	Honomanu	7/9/2013	20.86103	-156.16643	13.50	-
HMS-1	Coastal Spring	Honomanu	7/9/2013	20.86045	-156.16547	0.80	-
HMS-2	Coastal Spring	Honomanu	7/9/2013	20.86058	-156.16521	0.40	-
HMS-3	Coastal Spring	Honomanu	7/9/2013	20.85798	-156.16861	0.10	-
HMB-1	Marine	Honomanu	7/10/2013	20.86096	-156.16611	25.00	-
HMA-11	Marine	Honomanu	7/10/2013	20.86152	-156.16447	33.39	104
HMA-12	Marine	Honomanu	7/10/2013	20.86168	-156.16508	32.52	104.1
HMA-13	Marine	Honomanu	7/10/2013	20.86202	-156.16567	32.92	104.2
HMA-14	Marine	Honomanu	7/10/2013	20.86242	-156.16612	33.75	103.6
HMA-16	Marine	Honomanu	7/10/2013	20.86137	-156.16590	33.60	-
HMA-17	Marine	Honomanu	7/10/2013	20.86537	-156.16423	34.74	104.8
HMA-18	Marine	Honomanu	7/10/2013	20.86348	-156.16508	33.26	103.8
HMA-19	Marine	Honomanu	7/10/2013	20.86280	-156.16532	33.84	104.1
HMA-20	Marine	Honomanu	7/10/2013	20.86235	-156.16547	33.63	104.4
HMA-21	Stream	Honomanu	7/10/2013	20.86157	-156.16698	4.20	109.8
-	-	-	-	-	-	-	-
TVSP1	Coastal Spring	Kuau	4/4/2014	20.92492	-156.37111	7.88	90.4
TVP-1	Piezometer	Kuau	4/4/2014	20.92605	-156.36977	20.24	84.2
TVP-2	Piezometer	Kuau	4/4/2014	20.92510	-156.37097	1.80	89.4
TVM-2	Marine	Kuau	4/4/2014	20.92705	-156.37027	35.71	108.7
TVM-1	Marine	Kuau	4/4/2014	20.92640	-156.36978	33.95	111.5
TVS-1	Coastal Spring	Kuau	7/6/2013	20.92250	-156.37529	1.91	36.9
TVS-2	Coastal Spring	Kuau	7/6/2013	20.92211	-156.37637	1.10	42.7
TVS-3	Coastal Spring	Kuau	7/6/2013	20.92515	-156.37091	1.45	25.1
TVS-4	Coastal Spring	Kuau	7/6/2013	20.92354	-156.37221	1.38	36
TVP-1	Piezometer	Kuau	7/6/2013	20.92243	-156.37521	8.65	29.4
TVP-2	Piezometer	Kuau	7/6/2013	20.92257	-156.37379	4.77	36.4
TVP-3	Piezometer	Kuau	7/7/2013	20.92613	-156.36975	0.88	35.6
TVA-1	Marine	Kuau	7/8/2013	20.92255	-156.37508	31.18	96.2

Sample Name	Sample Type	Field Location	Date	Lat	Lon	Salinity	DO %
TVA-2	Marine	Kuau	7/8/2013	20.92283	-156.37433	32.82	81.1
TVA-3	Marine	Kuau	7/8/2013	20.92317	-156.37350	32.85	89.7
TVA-4	Marine	Kuau	7/8/2013	20.92430	-156.37173	32.06	125
TVA-5	Marine	Kuau	7/8/2013	20.92622	-156.37012	31.98	89
TVA-6	Marine	Kuau	7/8/2013	20.92278	-156.37535	28.01	107.5
TVA-7	Marine	Kuau	7/8/2013	20.92635	-156.37040	32.94	93.3
TVA-8	Marine	Kuau	7/8/2013	20.92652	-156.37090	32.89	97.8
TVA-9	Marine	Kuau	7/8/2013	20.92677	-156.37143	34.16	106.3
TVA-10	Marine	Kuau	7/8/2013	20.92723	-156.37257	34.74	88.5
-	-	-	-	-	-	-	-
HBW-1	Well	Honolua	4/1/2014	20.97382	-156.64310	0.40	101.7
HBW-2	Well	Honolua	4/1/2014	20.97679	-156.64040	0.29	101.8
HBW-3	Well	Honolua	4/1/2014	20.97833	-156.63972	0.15	103.1
NW1	Well	Waihee	7/16/2013	20.94416	-156.52284	0.12	-
KW1	Well	Waihee	7/16/2013	20.94899	-156.52020	0.12	-
MW	Well	Waiehu	7/16/2013	20.88824	-156.51205	0.34	-
WW	Well	Waihee	7/16/2013	20.90907	-156.51450	0.14	-
WH-2	Well	Waiehu	7/16/2013	20.90552	-156.50912	0.39	-
ITW	Well	Waiehu	7/16/2013	20.88286	-156.51302	0.12	-
KEP-W	Well	Waiehu	7/16/2013	20.88377	-156.53470	0.08	-
WAI-W	Well	Waiehu	7/16/2013	20.86120	-156.51483	0.16	-
PW	Well	Kuau	7/17/2013	20.84934	-156.30582	0.05	-
KAP-W	Well	Kuau	7/17/2013	20.88253	-156.29684	0.08	-
HAI-W	Well	Kuau	7/17/2013	20.89986	-156.32458	0.28	-
HW-2	Well	Honomanu	7/18/2013	20.84792	-156.13519	0.12	-
HBW-1	Well	Honolua	8/2/2012	20.97383	-156.64311	0.42	96.7
HBW-2	Well	Honolua	8/2/2012	20.98030	-156.63763	0.09	97.5
HBW-3	Well	Honolua	8/2/2012	20.97681	-156.64046	0.22	98.9

A 2. Nutrients and stable isotopes. Sample name, nutrient concentrations (μM), $\delta^{18}O$ value of H_2O (‰ vs VSMOW), and $\delta^{15}N$ and $\delta^{18}O$ values of NO_3^- (‰ vs AIR).

Sample Name	PO_4^{3-}	Si	N+N	NH_4^+	$\delta^{18}O$-H_2O	$\delta^{15}N$-NO_3^-	$\delta^{18}N$-NO_3^-
WC1	2.27	555.85	60.10	0.71	-4.28	12.81	8.85
WC2	1.29	657.27	108.18	5.83	-3.44	12.63	7.56
IST	0.44	311.14	0.71	0.59	-3.73	-	-
WM1	0.00	31.39	0.00	1.11	-	-	-
WM2	0.84	138.46	0.00	4.49	-1.62	-	-
WM3	0.00	3.03	0.00	0.85	-0.48	-	-
WP1	6.09	350.07	2.88	3.51	-3.27	13.91	11.01
WP2	1.97	406.94	0.31	1.99	-4.18	-	-
WB-ST	0.73	403.03	0.22	0.00	-3.69	-	-
WB-SP1	2.14	350.91	0.02	0.00	-3.24	-	-
WBP-1	2.61	233.24	3.19	0.01	-1.15	4.77	-0.96
WBP-2	0.64	69.30	3.17	0.00	-0.15	3.56	-0.32
WBP-3	8.36	209.92	0.03	0.00	-1.10	-	-
WBA-23	0.11	56.46	0.02	0.13	-0.75	-	-
WBA-24	0.13	40.79	0.04	0.04	-3.65	-	-
WBA-25	0.00	3.74	0.07	0.00	0.07	-	-
WBA-26	0.00	3.39	0.14	0.10	0.05	-	-
WBA-27	0.13	51.20	0.26	0.06	-0.37	-	-
WBA-28	0.13	50.04	0.07	0.00	-0.36	-	-
WBA-29	0.04	21.57	0.00	0.08	-0.01	-	-
WBA-30	0.04	21.06	0.11	0.13	0.08	-	-
WBA-31	0.00	14.31	0.00	0.08	0.03	-	-
WBA-32	0.00	4.23	0.06	0.08	0.07	-	-
-	-	-	-	-	-	-	-
KWP-9	1.21	244.96	14.36	1.38	-2.30	13.02	5.97
KWM-TS	0.35	48.26	1.23	0.95	-0.66	14.10	3.56
KWM-2	0.00	24.77	0.41	0.28	-0.54	-	-
KWM-3	0.00	16.31	0.25	0.33	-0.40	-	-
KWB-1	0.21	57.27	3.92	0.00	-0.32	-	-
KWB-2	0.43	101.81	11.03	0.00	-0.41	44.07	20.34
KWB-3	0.57	74.28	14.69	0.00	-0.37	31.40	14.52
KWB-4	0.21	57.63	3.70	0.00	-0.10	14.10	7.72
KWP-1	3.05	1067.97	91.31	0.00	-2.79	9.72	8.92
KWP-2	2.07	625.64	53.95	0.00	-2.38	11.68	1.65
KWP-3	2.13	397.31	29.20	0.00	-2.84	6.64	2.00
KWP-4	0.96	380.48	21.34	0.00	-1.81	15.93	4.76
KWP-5	1.18	241.50	2.36	115.98	-2.16	38.36	22.58
KWP-6	1.94	448.44	14.03	10.49	-0.37	10.27	1.41
KWP-7	1.80	343.69	17.96	0.21	-3.44	7.03	-1.68
KWP-8	2.25	720.41	5.34	0.00	-2.79	9.52	-3.78

Sample Name	PO_4^{3-}	Si	N+N	NH_4^+	$\delta^{18}O\text{-}H_2O$	$\delta^{15}N\text{-}NO_3^-$	$\delta^{18}N\text{-}NO_3^-$
KWA-X1	0.06	36.30	0.80	0.22	-0.08	-	-
KWA-TS	0.39	92.78	3.67	0.41	-0.39	34.61	19.77
KWA-14	0.45	86.00	1.09	0.64	0.02	-	-
KWA-17	1.00	152.74	3.01	4.48	0.05	22.15	14.57
KWA-18	0.03	14.51	0.94	0.06	-0.03	-	-
KWA-19	0.00	6.63	0.00	0.00	0.06	-	-
KWA-20	0.11	33.92	0.46	0.26	0.19	-	-
KWA-21	0.03	22.32	0.33	0.15	0.07	-	-
KWA-23	0.07	41.99	0.07	0.18	-0.02	-	-
KWA-24	0.41	96.78	1.33	0.19	-0.17	-	-
KWA-25	0.23	92.19	0.30	0.00	-0.06	-	-
KWA-26	0.19	64.79	1.16	0.00	-0.01	-	-
KWA-27	0.16	45.13	1.62	0.00	-0.15	-	-
KWA-28	0.01	15.19	0.05	0.00	-0.10	-	-
KWA-29	0.14	45.00	1.26	0.00	0.00	-	-
KWA-30	0.06	34.23	1.87	0.00	0.10	13.61	11.75
KWA-31	0.66	166.65	11.23	0.00	0.02	15.85	3.87
KWA-32	4.12	518.26	12.68	0.00	-0.37	16.86	14.60
Kan	0.84	347.18	0.30	8.73	-0.56	-	-
KWWTP	34.57	691.86	376.07	28.94	-2.62	21.38	11.25
-	-	-	-	-	-	-	-
MP1	8.53	610.98	258.49	0.00	-4.23	3.34	3.78
MP2	5.54	512.25	225.92	0.18	-3.41	1.87	0.21
MP3	7.48	570.82	298.43	1.24	-4.18	4.61	4.08
MP4	4.83	563.67	259.70	0.23	-4.02	3.52	3.39
MP5	1.07	54.66	21.38	0.09	-0.61	4.09	2.81
MM-1	0.00	0.66	0.68	0.35	-0.41	-	-
MM-2	0.19	19.20	11.51	1.34	-0.66	3.59	4.36
MM3	0.11	14.32	9.57	1.08	-0.62	3.76	4.38
MM4	0.00	0.21	0.24	0.33	-0.34	-	-
MM5	0.00	0.64	0.20	2.23	-0.32	-	-
MM6	0.00	0.00	0.00	0.08	-0.40	-	-
MM7	0.00	0.49	0.34	0.12	-0.39	-	-
MM8	0.65	52.40	47.80	4.40	-1.12	2.88	4.93
MM9	0.88	118.87	68.40	0.90	-1.22	1.67	3.13
MM10	0.23	47.42	27.27	1.01	-0.77	2.13	4.19
MM11	0.00	2.62	1.58	0.25	-0.41	3.05	4.45
MM12	0.00	0.87	0.09	0.18	-0.43		
MBP-1	2.41	191.54	131.82	0.00	-1.21	-	-
MBP-1A	2.42	206.28	135.04	0.00	-1.46	-	-
MBP-2	0.25	20.98	4.75	1.05	-0.14	-	-

Sample Name	PO_4^{3-}	Si	N+N	NH_4^+	$\delta^{18}O\text{-}H_2O$	$\delta^{15}N\text{-}NO_3^-$	$\delta^{18}N\text{-}NO_3^-$
MBP-3	0.26	17.50	9.20	0.00	0.23	-	-
MBP-4	0.50	62.11	7.01	2.10	-0.19	-	-
MBP-5	0.03	10.00	1.09	0.00	-0.07	-	-
MBP-6	1.19	57.77	3.91	0.00	-0.08	-	-
MBA-1	0.68	79.91	26.42	0.89	-0.35	-	-
MBA-2	0.15	23.34	7.34	0.03	-0.19	-	-
MBA-3	0.12	49.02	4.94	2.37	-0.14	-	-
MBB-1	0.28	56.98	17.19	0.30	-0.41	-	-
MBB-2	0.02	16.38	1.54	0.09	-0.11	-	-
MBB-3	0.00	3.42	0.00	0.00	-0.01	-	-
MBB-4	0.00	32.51	0.07	0.47	-0.03	-	-
MBC-1	0.82	85.70	33.50	0.44	-0.51	-	-
MBC-2	0.00	13.64	1.54	0.10	-0.07	-	-
MBC-3	0.00	3.11	0.00	0.02	-0.08	-	-
-	-	-	-	-	-	-	-
HP1	1.12	453.93	14.74	0.05	-3.63	4.78	4.14
HP2	1.49	476.44	14.84	0.00	-4.08	1.17	4.10
HP3	1.15	351.45	21.03	1.67	-4.10	1.68	4.09
HBSP1	1.03	272.98	22.79	2.00	-2.93	1.82	4.27
HBSP2	1.70	457.05	33.81	1.04	-4.53	1.71	5.07
HBSP3	2.23	411.40	33.33	0.76	-4.19	2.18	5.33
HBTS	0.22	83.29	3.04	0.06	-1.14	2.39	5.19
HBM-1	0.05	48.54	1.71	0.62	-0.85	1.20	4.00
HBM-2	0.00	13.14	0.03	4.04	-0.60	-	-
HBM-3	0.00	15.60	0.20	0.86	-0.58	-	-
HBM-4	0.00	7.13	0.00	1.34	-0.74	-	-
HBST	0.07	66.00	0.31	0.07	-4.14		
HBA-1	0.33	101.26	4.43	0.00	-1.35	-	-
HBA-1-5	0.24	78.29	3.38	0.23	-	-	-
HBA-2	0.07	40.25	1.48	0.50	-0.30	-	-
HBA-3	0.06	33.19	1.17	0.04	-	-	-
HBA-3-5	0.16	55.24	2.20	0.20	-0.17	-	-
HBA-4	0.02	24.27	0.86	-0.06	-0.20	-	-
HBA-5	0.00	23.52	0.27	0.41	-0.14	-	-
HBA-6	0.00	12.18	0.00	0.13	-0.05	-	-
HBM-1	0.21	37.22	3.46	0.73	-0.21	-	-
HBTS-1	0.00	9.88	0.08	0.00	-0.48	-	-
HBSP-A	1.79	489.96	38.20	0.52	-3.74	-	-
HBSP-B	2.53	489.74	34.75	0.00	-3.74	-	-
HBSP-C	0.80	242.08	8.30	0.00	-1.89	-	-

Sample Name	PO_4^{3-}	Si	N+N	NH_4^+	$\delta^{18}O\text{-}H_2O$	$\delta^{15}N\text{-}NO_3^-$	$\delta^{18}N\text{-}NO_3^-$
HMP-1	0.29	115.77	1.57	3.51	-3.49	1.23	0.44
HMSP1	2.06	543.72	6.12	0.16	-4.51	2.76	1.03
HMM1	0.29	112.40	0.38	0.86	-	-	-
HMM2	0.00	18.60	0.00	0.27	-0.62	-	-
HMST	0.41	168.88	1.83	0.16	-4.12	1.47	2.25
HMP-1	5.48	666.45	8.99	0.10	-4.59	0.93	-1.58
HMP-2	1.84	406.86	2.81	1.85	-2.99	2.28	3.11
HMS-1	4.37	782.15	8.54	0.45	-4.36	1.05	-1.70
HMS-2	4.38	778.81	8.29	0.45	-4.40	0.67	-1.93
HMS-3	3.27	846.16	8.35	0.00	-3.61	0.63	-1.94
HMB-1	1.03	218.41	0.92	0.08	2.29	-	-
HMA-11	0.33	56.82	0.43	0.00	-0.26	-	-
HMA-12	0.54	102.36	0.74	0.00	-0.49	-	-
HMA-13	0.29	49.80	0.23	0.00	-0.22	-	-
HMA-14	0.23	39.94	0.00	0.00	-0.23	-	-
HMA-16	0.19	38.59	0.03	0.10	-	-	-
HMA-17	0.10	15.71	0.00	0.00	-0.01	-	-
HMA-18	0.22	43.76	0.06	0.06	-0.25	-	-
HMA-19	0.23	42.71	0.07	0.01	-0.23	-	-
HMA-20	0.22	40.46	0.07	0.01	-0.20	-	-
HMA-21	3.29	851.23	7.78	0.00	-3.80	1.11	-0.54
-	-	-	-	-	-	-	-
TVSP1	3.52	699.44	289.22	2.48	-3.60	1.86	3.58
TVP-1	2.46	399.99	198.58	4.20	-2.26	1.78	3.98
TVP-2	2.37	806.21	383.77	1.15	-4.45	3.71	3.59
TVM-2	0.00	10.85	2.17	0.07	-	4.83	5.15
TVM-1	0.10	47.88	15.48	0.34	-0.66	3.61	5.80
TVS-1	4.59	849.89	460.84	0.00	-3.80	2.86	2.38
TVS-2	6.68	899.01	415.66	0.00	-3.78	3.43	3.26
TVS-3	5.41	812.99	422.83	1.68	-3.96	3.44	3.65
TVS-4	4.14	823.53	403.32	0.00	-3.91	2.83	3.00
TVP-1	4.05	721.83	351.71	0.97	-1.80	3.36	3.66
TVP-2	5.66	775.11	390.20	0.00	-4.29	2.94	2.98
TVP-3	3.73	813.36	456.95	0.00	-3.94	2.92	3.12
TVA-1	0.72	110.68	40.61	0.11	-0.27	3.38	4.36
TVA-2	0.42	62.70	23.11	0.21	-0.15	3.18	4.02
TVA-3	0.69	104.56	38.57	0.14	-0.41	2.98	3.50
TVA-4	0.15	53.53	14.99	0.20	-0.05	4.16	5.35
TVA-5	0.29	66.82	22.92	0.30	-0.33	3.63	4.38
TVA-6	0.64	197.96	59.62	1.27	-0.53	3.98	4.17
TVA-7	0.39	79.07	28.20	0.31	-0.21	3.33	3.74

Sample Name	PO_4^{3-}	Si	N+N	NH_4^+	$\delta^{18}O\text{-}H_2O$	$\delta^{15}N\text{-}NO_3^-$	$\delta^{18}N\text{-}NO_3^-$
TVA-8	0.27	63.22	19.73	0.14	-0.12	3.67	4.80
TVA-9	0.08	19.29	5.25	0.00	-0.04	3.59	4.21
TVA-10	0.04	4.22	0.78	0.00	-0.10	-	-
-	-	-	-	-	-	-	-
Nap-A	2.78	685.04	31.53	0.00	-3.95	2.51	4.76
Nap-C	2.41	652.30	16.35	0.06	-3.94	3.52	2.57
Hon-B	2.16	583.21	16.08	0.03	-4.06	2.95	1.95
NW1	6.23	860.45	49.46	0.00	-3.83	1.03	2.03
KW1	4.32	805.97	11.13	0.00	-3.88	1.13	0.28
MW	2.98	896.41	33.01	0.00	-3.89	1.97	2.54
WW	3.41	776.87	28.55	0.05	-3.79	1.65	2.75
WH-2	3.87	899.18	21.55	0.00	-3.93	1.64	3.19
ITW	2.49	778.86	26.21	0.00	-3.68	6.37	4.13
KEP-W	2.28	780.11	10.69	0.00	-2.76	3.11	-0.43
WAI-W	4.74	884.66	35.75	0.08	-3.97	1.76	1.58
PW	1.93	610.19	23.06	0.00	-5.35	2.85	1.27
KAP-W	2.49	820.87	29.47	0.00	-4.33	3.87	4.94
HAI-W	2.43	787.90	94.38	0.00	-3.80	3.96	5.00
HW-2	2.72	773.05	7.48	0.01	-4.84	0.27	-2.41
HBW-1	2.58	722.49	19.97	0.00	-3.55	-	-
HBW-2	2.41	612.80	25.23	0.00	-3.72	0.27	-3.78
HBW-3	2.60	681.96	18.86	0.00	-3.70	-	-

A 3. Data collected during radon time series from each of the field areas. Temperature, salinity, and mixed layer depth are average values measured over 30 minute intervals.

Field Area	Date/time	Water Temp (°c)	Salinity	Rn activity in air (Bq/m^3)	Error-2sigma (Bq/m^3)	Wind Speed (m/s)	Mixed layer depth (cm)
Kuau	7/12/2013 10:48	25.2	32.2	1037.6	112.9	5.4	35
Kuau	7/12/2013 11:18	25.3	32.4	1397.4	130.1	5.8	38
Kuau	7/12/2013 11:48	25.4	32.5	1574.3	137.9	5.4	39
Kuau	7/12/2013 12:18	25.6	32.5	1402.1	130.4	4.9	43
Kuau	7/12/2013 12:48	25.7	32.6	1336.6	127.8	4.2	47
Kuau	7/12/2013 13:18	25.7	33.0	1226.4	122.4	3.6	52
Kuau	7/12/2013 13:48	25.8	33.1	1164.4	120.1	4.2	60
Kuau	7/12/2013 14:18	25.9	33.4	870.8	104.3	4.9	68
Kuau	7/12/2013 14:48	25.8	33.8	625.9	89.9	3.8	75
Kuau	7/12/2013 15:18	25.9	33.7	450.1	76.6	2.7	83
Kuau	7/12/2013 15:48	25.9	33.8	402.0	72.8	4.9	87
Kuau	7/12/2013 16:18	25.8	34.0	401.6	72.7	7.2	91
Kuau	7/12/2013 16:48	25.7	34.0	494.7	80.0	6.9	94
Kuau	7/12/2013 17:18	25.5	34.0	670.0	92.0	6.7	94

Field Area	Date/time	Water Temp (°c)	Salinity	Rn activity in air (Bq/m^3)	Error-2sigma (Bq/m^3)	Wind Speed (m/s)	Mixed layer depth (cm)
Kuau	7/12/2013 17:48	25.4	34.0	674.0	92.3	6.7	94
Kuau	7/12/2013 18:18	25.3	34.0	639.6	90.1	6.7	92
Kuau	7/12/2013 18:48	25.2	33.9	652.8	91.4	8.3	89
Kuau	7/12/2013 19:18	25.1	33.7	794.4	99.9	9.8	86
Kuau	7/12/2013 19:48	25.0	33.5	742.1	96.5	10.7	80
Kuau	7/12/2013 20:18	25.0	33.4	842.5	102.8	11.6	75
Kuau	7/12/2013 20:48	24.9	33.2	1017.9	112.0	12.1	69
Kuau	7/12/2013 21:18	24.9	33.1	974.0	109.7	12.5	63
Kuau	7/12/2013 21:48	24.8	32.9	1259.7	123.9	11.0	59
Kuau	7/12/2013 22:18	24.8	32.7	1350.4	128.1	9.4	54
Kuau	7/12/2013 22:48	24.7	32.5	1429.6	131.9	9.8	50
Kuau	7/12/2013 23:18	24.7	32.4	1510.2	135.6	10.3	48
Kuau	7/12/2013 23:48	24.7	32.2	1558.5	137.6	10.3	46
Kuau	7/13/2013 0:18	24.6	32.3	1530.9	136.3	10.3	46
Kuau	7/13/2013 0:48	24.6	32.3	1715.2	143.7	10.5	46
Kuau	7/13/2013 1:18	24.6	32.3	1666.9	141.7	10.7	47
Kuau	7/13/2013 1:48	24.6	32.5	1684.1	142.9	10.1	49
Kuau	7/13/2013 2:18	24.6	32.5	1528.8	136.3	9.4	53
Kuau	7/13/2013 2:48	24.6	32.6	1577.2	138.0	8.7	56
Kuau	7/13/2013 3:18	24.6	32.8	1444.7	132.8	8.0	60
Kuau	7/13/2013 3:48	24.7	32.9	1444.7	132.6	7.6	63
Kuau	7/13/2013 4:18	24.7	33.0	1274.6	125.0	7.2	66
Kuau	7/13/2013 4:48	24.7	33.2	1250.5	124.5	6.5	69
Kuau	7/13/2013 5:18	24.7	33.2	1171.3	119.9	5.8	71
Kuau	7/13/2013 5:48	24.7	33.3	1133.4	118.2	7.4	71
Kuau	7/13/2013 6:18	24.7	33.2	1077.3	115.2	8.9	71
Kuau	7/13/2013 6:48	24.7	33.3	1094.5	116.1	7.8	70
Kuau	7/13/2013 7:18	24.7	33.2	1229.8	122.5	6.7	69
Kuau	7/13/2013 7:48	24.7	33.3	1135.8	118.1	6.3	68
Kuau	7/13/2013 8:18	24.8	33.1	1174.7	119.9	5.8	66
Kuau	7/13/2013 8:48	24.9	33.1	1198.8	121.2	5.1	63
Kuau	7/13/2013 9:18	25.0	33.1	1219.5	122.2	4.5	56
-	-	-	-	-	-	-	-
Maalaea	3/30/2014 9:49	24.8	33.1	201.8	57.1	4.9	38
Maalaea	3/30/2014 10:19	25.2	33.2	763.9	105.0	5.4	41
Maalaea	3/30/2014 10:49	25.4	33.5	1046.0	121.7	5.8	47
Maalaea	3/30/2014 11:19	25.6	33.9	950.9	116.3	4.2	50
Maalaea	3/30/2014 11:49	25.9	34.1	996.2	119.0	2.7	57
Maalaea	3/30/2014 12:19	26.1	34.1	818.5	108.5	2.0	65
Maalaea	3/30/2014 12:49	26.3	34.1	707.5	101.3	1.3	73

Field Area	Date/time	Water Temp (°c)	Salinity	Rn activity in air (Bq/m^3)	Error-2sigma (Bq/m^3)	Wind Speed (m/s)	Mixed layer depth (cm)
Maalaea	3/30/2014 13:19	26.3	34.2	748.7	104.2	3.1	81
Maalaea	3/30/2014 13:49	26.6	33.9	570.6	91.9	4.9	88
Maalaea	3/30/2014 14:19	26.8	33.7	632.3	96.2	3.1	93
Maalaea	3/30/2014 14:49	26.8	33.6	629.1	96.2	1.3	100
Maalaea	3/30/2014 15:19	26.8	33.7	675.9	98.9	2.0	103
Maalaea	3/30/2014 15:49	26.8	33.8	606.4	94.1	2.7	108
Maalaea	3/30/2014 16:19	26.7	33.9	546.4	89.9	1.3	107
Maalaea	3/30/2014 16:49	26.7	33.9	720.1	101.9	0.0	108
Maalaea	3/30/2014 17:19	26.7	34.0	590.6	92.9	0.0	104
Maalaea	3/30/2014 17:49	26.5	34.1	675.9	99.4	0.0	100
Maalaea	3/30/2014 18:19	26.4	34.2	625.4	95.7	0.0	96
Maalaea	3/30/2014 18:49	26.2	34.3	682.8	99.7	0.0	90
Maalaea	3/30/2014 19:19	26.0	34.3	698.0	100.4	0.7	82
Maalaea	3/30/2014 19:49	25.8	34.5	735.9	102.9	1.3	75
Maalaea	3/30/2014 20:19	25.7	34.3	720.8	102.2	6.3	68
Maalaea	3/30/2014 20:49	25.6	34.3	628.5	96.1	7.6	62
Maalaea	3/30/2014 21:19	25.4	34.1	727.1	102.6	7.6	57
Maalaea	3/30/2014 21:49	25.3	34.1	752.4	104.1	7.6	54
Maalaea	3/30/2014 22:19	25.0	33.4	872.5	111.6	7.6	52
Maalaea	3/30/2014 22:49	24.8	33.3	891.5	112.7	7.6	52
Maalaea	3/30/2014 23:19	24.7	32.7	1040.1	121.2	7.6	54
Maalaea	3/30/2014 23:49	24.6	32.9	1091.6	124.2	7.6	57
Maalaea	3/31/2014 0:19	24.4	32.8	1240.3	131.8	7.6	62
Maalaea	3/31/2014 0:49	24.3	32.8	1235.1	131.6	7.6	68
Maalaea	3/31/2014 1:19	24.2	32.4	1260.5	132.9	7.8	74
Maalaea	3/31/2014 1:49	24.1	32.6	1257.3	132.9	8.0	80
Maalaea	3/31/2014 2:19	24.0	32.3	1149.6	127.7	7.6	88
Maalaea	3/31/2014 2:49	24.0	32.3	1143.3	127.2	7.2	92
Maalaea	3/31/2014 3:19	23.9	32.5	1437.8	141.4	5.6	97
Maalaea	3/31/2014 3:49	23.9	32.3	1177.1	128.7	4.0	98
Maalaea	3/31/2014 4:19	23.9	32.4	1168.6	128.2	5.4	98
Maalaea	3/31/2014 4:49	23.9	32.5	1168.6	128.7	6.7	98
Maalaea	3/31/2014 5:19	23.8	32.6	1060.0	122.3	6.9	96
Maalaea	3/31/2014 5:49	23.8	32.7	1098.9	124.7	7.2	91
Maalaea	3/31/2014 6:19	23.8	32.8	1132.8	126.4	5.1	86
Maalaea	3/31/2014 6:49	23.9	32.9	1263.6	133.5	3.1	79
Maalaea	3/31/2014 7:19	23.8	33.0	1225.6	131.1	3.1	72
Maalaea	3/31/2014 7:49	23.8	32.9	1187.6	129.3	3.1	65
Maalaea	3/31/2014 8:19	24.0	33.1	1203.4	130.0	2.9	57
Maalaea	3/31/2014 8:49	24.1	33.0	1146.4	127.0	2.7	52

Field Area	Date/time	Water Temp (°c)	Salinity	Rn activity in air (Bq/m^3)	Error-2sigma (Bq/m^3)	Wind Speed (m/s)	Mixed layer depth (cm)
Maalaea	3/31/2014 9:19	24.2	32.7	1358.6	137.8	3.4	46
Maalaea	3/31/2014 9:49	24.24352	32.8	1228.8	131.4	4.0	36
-	-	-	-	-	-	-	-
Kahului	3/28/2014 18:22	26.3	32.8	107.3	43.6	0.0	69
Kahului	3/28/2014 18:52	26.3	32.9	202.1	57.6	0.0	72
Kahului	3/28/2014 19:22	26.3	33.0	186.5	55.3	0.0	71
Kahului	3/28/2014 19:52	26.2	33.0	199.2	56.9	2.2	72
Kahului	3/28/2014 20:22	26.1	33.2	221.5	59.7	2.9	74
Kahului	3/28/2014 20:52	26.1	33.1	199.3	57.0	3.6	79
Kahului	3/28/2014 21:22	26.0	33.2	176.7	54.0	4.0	86
Kahului	3/28/2014 21:52	26.0	33.2	142.0	49.6	4.5	92
Kahului	3/28/2014 22:22	26.0	33.3	110.4	44.2	3.4	100
Kahului	3/28/2014 22:52	26.0	33.4	135.7	48.2	2.2	109
Kahului	3/28/2014 23:22	25.9	33.5	142.0	49.1	1.3	117
Kahului	3/28/2014 23:52	25.9	33.5	170.4	53.5	2.7	124
Kahului	3/29/2014 0:22	25.9	33.6	135.8	48.2	3.6	130
Kahului	3/29/2014 0:52	25.9	33.7	154.6	50.9	1.3	135
Kahului	3/29/2014 1:22	25.9	33.6	138.8	49.1	2.0	137
Kahului	3/29/2014 1:52	25.8	33.6	123.2	46.3	2.7	134
Kahului	3/29/2014 2:22	25.8	33.7	135.8	48.2	3.1	127
Kahului	3/29/2014 2:52	25.8	33.6	157.8	52.3	3.6	121
Kahului	3/29/2014 3:22	25.7	33.6	113.6	44.7	3.1	117
Kahului	3/29/2014 3:52	25.7	33.5	154.6	50.9	2.7	112
Kahului	3/29/2014 4:22	25.6	33.4	135.8	48.2	2.7	103
Kahului	3/29/2014 4:52	25.6	33.3	142.0	49.1	2.7	96
Kahului	3/29/2014 5:22	25.6	33.2	142.1	50.1	2.5	89
Kahului	3/29/2014 5:52	25.5	33.0	182.9	55.1	2.2	80
Kahului	3/29/2014 6:22	25.4	32.9	164.1	52.3	2.7	72
Kahului	3/29/2014 6:52	25.4	32.9	148.3	50.0	3.1	66
Kahului	3/29/2014 7:22	25.4	32.9	132.7	48.2	2.2	60
Kahului	3/29/2014 7:52	25.4	32.8	63.2	35.9	1.3	58
Kahului	3/29/2014 8:22	25.3	32.9	63.1	35.2	2.2	59
Kahului	3/29/2014 8:52	25.3	32.9	69.5	36.6	3.1	60
Kahului	3/29/2014 9:22	25.3	33.0	75.7	38.5	3.4	66
Kahului	3/29/2014 9:52	25.4	33.1	69.5	36.6	3.6	70
Kahului	3/29/2014 10:22	25.5	33.2	60.0	35.3	1.8	78
Kahului	3/29/2014 10:52	25.6	33.3	75.9	39.2	0.0	87
Kahului	3/29/2014 11:22	25.7	33.5	66.3	36.6	0.0	98
Kahului	3/29/2014 11:52	25.8	33.6	34.7	28.2	0.0	103
Kahului	3/29/2014 12:22	25.8	33.8	37.9	30.8	0.0	110

Field Area	Date/time	Water Temp (°c)	Salinity	Rn activity in air (Bq/m^3)	Error-2sigma (Bq/m^3)	Wind Speed (m/s)	Mixed layer depth (cm)
Kahului	3/29/2014 12:52	25.9	33.9	15.8	21.8	0.0	118
Kahului	3/29/2014 13:22	25.9	33.9	19.0	23.1	1.1	123
Kahului	3/29/2014 13:52	25.8	34.0	28.5	26.3	2.2	129
Kahului	3/29/2014 14:22	26.0	33.9	25.3	25.3	2.7	131
Kahului	3/29/2014 14:52	26.1	33.8	15.8	21.8	3.1	133
Kahului	3/29/2014 15:22	26.0	33.8	19.0	24.2	2.9	128
Kahului	3/29/2014 15:52	26.0	33.8	25.3	26.3	2.7	121
Kahului	3/29/2014 16:22	26.0	33.7	6.3	19.0	2.7	115
Kahului	3/29/2014 16:52	26.0	33.6	15.8	21.8	2.7	107
Kahului	3/29/2014 17:22	26.0	33.4	15.8	23.1	2.5	99
-	-	-	-	-	-	-	-
Honolua	3/31/2014 17:14	24.7	34.8	91.4	42.0	5.1	63
Honolua	3/31/2014 17:44	24.7	34.7	132.7	49.2	5.8	62
Honolua	3/31/2014 18:14	24.6	34.4	253.1	63.3	5.4	57
Honolua	3/31/2014 18:44	24.5	34.1	243.9	62.3	4.9	51
Honolua	3/31/2014 19:14	24.4	33.5	389.5	77.1	4.9	45
Honolua	3/31/2014 19:44	24.3	33.2	399.0	77.7	4.9	39
Honolua	3/31/2014 20:14	24.2	32.8	557.4	90.8	5.8	33
Honolua	3/31/2014 20:44	24.1	32.3	563.7	91.1	7.2	28
Honolua	3/31/2014 21:14	24.0	32.2	753.7	104.9	7.6	24
Honolua	3/31/2014 21:44	24.0	31.9	913.6	114.0	8.0	22
Honolua	3/31/2014 22:14	24.0	31.9	1009.4	119.9	7.6	21
Honolua	3/31/2014 22:44	23.9	32.0	1050.5	122.3	7.2	21
Honolua	3/31/2014 23:14	23.8	31.9	1066.3	123.0	7.4	23
Honolua	3/31/2014 23:44	23.9	32.2	1082.1	124.0	7.6	27
Honolua	4/1/2014 0:14	23.9	32.4	1060.0	122.8	7.4	32
Honolua	4/1/2014 0:44	23.9	32.7	1063.2	122.7	7.6	36
Honolua	4/1/2014 1:14	24.0	33.1	980.9	118.1	5.4	41
Honolua	4/1/2014 1:44	24.1	33.5	886.0	113.0	3.6	45
Honolua	4/1/2014 2:14	24.1	33.6	705.0	101.2	3.1	48
Honolua	4/1/2014 2:44	24.1	33.8	689.2	99.9	2.7	49
Honolua	4/1/2014 3:14	24.1	33.9	562.2	91.5	2.9	51
Honolua	4/1/2014 3:44	24.1	33.8	549.6	90.6	3.1	51
Honolua	4/1/2014 4:14	24.1	33.8	521.2	87.7	6.9	50
Honolua	4/1/2014 4:44	24.1	33.8	473.8	84.7	6.3	49
Honolua	4/1/2014 5:14	24.0	33.3	492.7	85.7	7.2	45
Honolua	4/1/2014 5:44	24.0	33.3	641.2	96.5	8.0	41
Honolua	4/1/2014 6:14	23.9	32.8	675.9	99.2	6.5	35
Honolua	4/1/2014 6:44	23.9	32.5	758.7	104.5	4.9	29
Honolua	4/1/2014 7:14	23.8	32.1	878.8	112.1	5.6	23

Field Area	Date/time	Water Temp (°c)	Salinity	Rn activity in air (Bq/m^3)	Error-2sigma (Bq/m^3)	Wind Speed (m/s)	Mixed layer depth (cm)
Honolua	4/1/2014 7:44	23.7	31.5	1036.9	121.2	6.3	15
Honolua	4/1/2014 8:14	23.6	31.0	1081.2	123.9	5.6	9
Honolua	4/1/2014 8:44	23.6	30.6	1104.3	125.1	4.9	3
Honolua	4/1/2014 9:14	23.6	30.6	1275.1	134.0	4.7	1
Honolua	4/1/2014 9:44	23.6	30.4	1493.0	144.9	5.6	0
Honolua	4/1/2014 10:14	23.6	30.3	1451.8	143.0	5.6	0
Honolua	4/1/2014 10:44	23.7	30.6	1480.3	143.5	6.7	1
Honolua	4/1/2014 11:14	23.8	31.0	1534.2	146.8	5.6	6
Honolua	4/1/2014 11:44	23.9	31.5	1451.8	142.5	4.5	11
Honolua	4/1/2014 12:14	23.9	31.8	1518.3	145.5	5.4	20
Honolua	4/1/2014 12:44	24.0	32.2	1304.8	135.2	6.3	28
Honolua	4/1/2014 13:14	24.2	33.1	1223.5	131.9	6.0	38
Honolua	4/1/2014 13:44	24.2	33.6	1010.3	120.3	5.8	45
Honolua	4/1/2014 14:14	24.3	34.0	879.6	112.6	5.8	53
Honolua	4/1/2014 14:44	24.4	34.1	813.2	108.0	5.8	59
Honolua	4/1/2014 15:14	24.4	34.4	679.7	99.7	6.0	64
Honolua	4/1/2014 15:44	24.5	34.6	575.4	92.6	6.3	68
Honolua	4/1/2014 16:14	24.5	34.6	334.8	72.9	7.6	71
-	-	-	-	-	-	-	-
Waiehu	3/27/2014 9:33	24.6	31.5	34.7	28.1	2.7	55
Waiehu	3/27/2014 10:03	25.0	31.2	66.2	35.9	2.2	62
Waiehu	3/27/2014 10:33	25.2	32.3	69.4	36.6	2.2	69
Waiehu	3/27/2014 11:03	25.4	33.1	85.2	39.7	2.2	74
Waiehu	3/27/2014 11:33	25.6	34.0	91.5	40.9	2.7	79
Waiehu	3/27/2014 12:03	25.8	34.0	72.6	37.2	3.1	82
Waiehu	3/27/2014 12:33	25.9	34.4	66.3	35.9	3.1	85
Waiehu	3/27/2014 13:03	26.1	34.2	47.3	31.6	3.1	84
Waiehu	3/27/2014 13:33	26.3	34.2	44.2	30.8	2.2	83
Waiehu	3/27/2014 14:03	26.6	33.7	41.1	30.0	1.3	80
Waiehu	3/27/2014 14:33	26.7	33.7	60.0	34.6	2.0	75
Waiehu	3/27/2014 15:03	26.6	33.3	53.7	33.1	2.7	68
Waiehu	3/27/2014 15:33	26.4	33.2	38.0	29.1	2.5	62
Waiehu	3/27/2014 16:03	26.0	29.9	75.8	37.9	2.2	55
Waiehu	3/27/2014 16:33	25.6	30.0	41.1	30.0	2.2	48
Waiehu	3/27/2014 17:03	24.9	25.9	34.8	28.3	1.3	43
Waiehu	3/27/2014 17:33	24.3	21.7	63.2	35.3	0.7	37
Waiehu	3/27/2014 18:03	24.1	21.2	82.1	39.1	0.0	34
Waiehu	3/27/2014 18:33	23.7	19.5	66.3	35.9	1.6	32
Waiehu	3/27/2014 19:03	24.0	22.3	63.2	35.3	3.1	32
Waiehu	3/27/2014 19:33	24.1	24.3	101.1	42.6	1.6	33

Field Area	Date/time	Water Temp (°c)	Salinity	Rn activity in air (Bq/m^3)	Error-2sigma (Bq/m^3)	Wind Speed (m/s)	Mixed layer depth (cm)
Waiehu	3/27/2014 20:03	24.5	27.4	79.0	38.6	0.0	35
Waiehu	3/27/2014 20:33	24.8	30.1	104.2	43.2	0.0	39
Waiehu	3/27/2014 21:03	25.0	32.1	88.4	40.3	0.0	43
Waiehu	3/27/2014 21:33	25.0	33.0	72.6	37.3	1.6	47
Waiehu	3/27/2014 22:03	25.0	32.6	85.3	40.3	3.1	53
Waiehu	3/27/2014 22:33	25.0	32.7	69.5	36.6	1.6	59
Waiehu	3/27/2014 23:03	25.0	32.9	50.5	32.4	0.0	67
Waiehu	3/27/2014 23:33	25.0	32.8	37.9	30.0	5.8	75
Waiehu	3/28/2014 0:03	25.0	33.0	47.4	33.1	6.5	87
Waiehu	3/28/2014 0:33	24.9	32.9	37.9	29.1	4.9	91
Waiehu	3/28/2014 1:03	24.8	32.6	34.8	28.2	2.7	99
Waiehu	3/28/2014 1:33	24.6	32.2	28.5	26.3	6.7	97
Waiehu	3/28/2014 2:03	24.6	32.8	31.6	27.3	5.8	92
Waiehu	3/28/2014 2:33	24.4	32.6	44.3	30.8	4.2	83
-	-	-	-	-	-	-	-
Honomanu	4/2/2014 11:30	21.5	2.6	369.5	75.2	6.0	43
Honomanu	4/2/2014 12:00	21.7	4.7	533.8	88.9	6.3	48
Honomanu	4/2/2014 12:30	22.1	8.7	521.6	87.8	6.5	56
Honomanu	4/2/2014 13:00	22.7	15.0	521.6	87.8	6.7	64
Honomanu	4/2/2014 13:30	23.1	18.5	493.2	86.3	6.7	72
Honomanu	4/2/2014 14:00	23.6	22.7	423.6	80.6	6.7	86
Honomanu	4/2/2014 14:30	23.8	25.3	382.5	76.7	5.4	89
Honomanu	4/2/2014 15:00	23.6	24.8	350.9	73.2	4.0	98
Honomanu	4/2/2014 15:30	23.5	23.8	299.5	68.4	4.9	101
Honomanu	4/2/2014 16:00	23.5	23.2	318.4	70.0	5.8	105
Honomanu	4/2/2014 16:30	23.5	24.8	350.0	73.3	6.0	111
Honomanu	4/2/2014 17:00	23.7	27.8	293.2	67.4	6.3	117
Honomanu	4/2/2014 17:30	23.6	27.3	271.1	65.1	6.7	114
Honomanu	4/2/2014 18:00	23.6	28.1	321.6	70.3	7.2	110
Honomanu	4/2/2014 18:30	23.5	28.6	305.8	68.7	8.5	106
Honomanu	4/2/2014 19:00	23.5	29.5	362.6	74.5	9.8	104
Honomanu	4/2/2014 19:30	23.5	29.7	334.2	72.4	9.8	97
Honomanu	4/2/2014 20:00	23.5	30.0	353.1	73.3	9.8	92
Honomanu	4/2/2014 20:30	23.3	29.2	403.6	77.9	9.8	86
Honomanu	4/2/2014 21:00	23.3	29.5	463.5	83.5	9.8	80
Honomanu	4/2/2014 21:30	23.3	29.6	501.8	86.6	9.6	76
Honomanu	4/2/2014 22:00	23.3	30.1	460.7	82.8	9.4	72
Honomanu	4/2/2014 22:30	23.3	30.0	510.8	86.8	9.6	71
Honomanu	4/2/2014 23:00	23.1	27.6	472.9	83.8	9.8	69
Honomanu	4/2/2014 23:30	22.6	22.8	533.3	88.6	10.1	69

Field Area	Date/time	Water Temp (°c)	Salinity	Rn activity in air (Bq/m^3)	Error-2sigma (Bq/m^3)	Wind Speed (m/s)	Mixed layer depth (cm)
Honomanu	4/3/2014 0:00	22.0	17.2	574.3	91.9	10.3	69
Honomanu	4/3/2014 0:30	21.2	7.3	941.2	115.7	9.6	73
Honomanu	4/3/2014 1:00	21.0	4.0	1302.5	134.8	8.9	75
Honomanu	4/3/2014 1:30	20.9	4.3	891.5	112.7	9.6	79
Honomanu	4/3/2014 2:00	20.8	5.6	562.2	91.5	10.3	80
Honomanu	4/3/2014 2:30	20.6	4.8	505.4	86.5	9.8	84
Honomanu	4/3/2014 3:00	20.6	5.3	369.2	75.4	9.4	85
Honomanu	4/3/2014 3:30	20.6	7.1	356.6	74.0	9.8	89
Honomanu	4/3/2014 4:00	20.7	8.0	403.9	79.1	10.3	91
Honomanu	4/3/2014 4:30	20.9	10.7	327.9	71.2	9.6	90
Honomanu	4/3/2014 5:00	21.0	11.8	368.9	75.7	8.9	86
Honomanu	4/3/2014 5:30	21.0	12.5	356.3	74.2	8.0	84
Honomanu	4/3/2014 6:00	21.1	13.0	375.2	75.4	7.2	81
Honomanu	4/3/2014 6:30	21.2	14.3	425.6	79.8	6.9	74
Honomanu	4/3/2014 7:00	21.2	13.8	463.5	83.0	6.7	72
Honomanu	4/3/2014 7:30	20.6	7.9	479.7	84.4	7.4	65
Honomanu	4/3/2014 8:00	20.3	4.8	549.1	89.8	8.0	58
Honomanu	4/3/2014 8:30	20.4	6.1	527.0	88.1	7.8	49
Honomanu	4/3/2014 9:00	20.6	6.0	583.8	92.8	7.6	46
Honomanu	4/3/2014 9:30	21.2	9.7	735.9	103.2	7.8	43
Honomanu	4/3/2014 10:00	21.7	11.6	615.4	94.9	8.0	42
Honomanu	4/3/2014 10:30	22.2	12.3	602.7	94.4	8.9	42
Honomanu	4/3/2014 11:00	22.6	15.1	549.1	90.0	6.7	43
Honomanu	4/3/2014 11:30	23.1	18.4	615.9	94.8	7.6	44

A 4. Data collected during radon surface water surveys. Salinity and water temperature (Temp) average values measured over 5 minute intervals. Mixed layer depths were determined from periodic salinity depth profiling.

Field Area	Latitude	Longitude	Date/Time	Mixed layer depth (cm)	Surface Area (m^2)	Shoreline Length (m)	Salinity	Water Temp (°c)	Rn activity in air (Bq/m^3)	Wind Speed (m/s)
Kuau	20.92297	-156.37349	7/12/2013 7:11	1.0	7553	77	33.9	24.3	103.1	7.2
Kuau	20.92435	-156.37261	7/12/2013 7:16	0.7	6841	251	34.2	24.4	123.7	7.3
Kuau	20.92422	-156.37184	7/12/2013 7:21	0.6	3760	101	34.3	24.4	185.5	7.3
Kuau	20.92545	-156.37161	7/12/2013 7:26	0.6	5067	169	34.6	24.4	247.4	7.3
Kuau	20.92621	-156.37106	7/12/2013 7:31	0.6	7757	116	33.7	24.3	474.1	7.4
Kuau	20.92649	-156.37019	7/12/2013 7:36	0.6	5075	89	34.5	24.2	494.7	7.4
Kuau	20.92720	-156.37077	7/12/2013 7:41	0.6	2255	143	34.7	24.1	371.1	7.5
Kuau	20.92798	-156.37066	7/12/2013 7:46	0.6	1243	20	34.8	24.1	432.9	7.5
Kuau	20.92296	-156.37508	7/12/2013 8:31	1.2	5420	178	34.0	24.3	309.2	7
Kuau	20.92445	-156.37672	7/12/2013 8:36	0.3	26301	179	34.8	24.3	103.1	6.8
Kuau	20.92235	-156.37699	7/12/2013 8:41	0.8	22948	161	34.7	24.4	268.0	6.7
Kuau	20.92165	-156.37829	7/12/2013 8:46	0.9	5767	273	34.6	24.4	185.5	6.6
Kuau	20.92061	-156.37843	7/12/2013 8:51	0.9	5983	178	34.3	24.5	206.1	6.5
Kuau	20.91977	-156.37942	7/12/2013 8:56	0.9	6444	293	34.5	24.8	268.0	6.4
Kuau	20.92020	-156.38169	7/12/2013 9:01	0.6	11081	219	34.6	24.6	474.1	6.3
Kuau	20.91843	-156.38148	7/12/2013 9:06	0.6	11993	293	33.9	24.6	268.0	6.3
Kuau	20.91752	-156.38291	7/12/2013 9:11	0.6	17836	219	34.1	24.8	371.1	6.3
-	-	-	-	-	-		-	-	-	-
Maalaea	20.79177	-156.50947	4/30/2014 11:19	0.6	1024	21	32.6	24.9	571.1	4.8
Maalaea	20.79195	-156.50951	4/30/2014 11:24	0.6	656	21	32.3	25.0	666.3	4.2
Maalaea	20.79229	-156.50877	4/30/2014 11:29	0.7	3090	87	30.6	25.1	723.4	3.6
Maalaea	20.79387	-156.50761	4/30/2014 11:34	0.7	7624	208	30.5	25.0	1085.0	3
Maalaea	20.79547	-156.50547	4/30/2014 12:09	0.6	4539	183	33.2	25.6	1588.5	0.4
Maalaea	20.79593	-156.50350	4/30/2014 12:14	0.2	2755	213	34.6	25.5	1741.6	0.6
Maalaea	20.79599	-156.50119	4/30/2014 12:19	0.0	9619	265	35.1	25.3	1332.5	0.7

Field Area	Latitude	Longitude	Date/Time	Mixed layer depth (cm)	Surface Area (m^2)	Shoreline Length (m)	Salinity	Water Temp (°c)	Rn activity in air (Bq/m^3)	Wind Speed (m/s)
Maalaea	20.79656	-156.50037	4/30/2014 12:24	0.0	n/a	92	35.4	25.3	913.7	1
Maalaea	20.79652	-156.49936	4/30/2014 12:29	0.0	n/a	118	35.4	25.3	514.0	1.3
Maalaea	20.79693	-156.49776	4/30/2014 12:34	0.0	n/a	173	35.5	25.3	323.6	1.5
Maalaea	20.79621	-156.49772	4/30/2014 12:39	0.2	10699	180	34.4	25.1	494.9	1.7
-	-	-	-	-	-		-	-	-	-
Kahului	20.89788	-156.46320	7/20/2013 9:21	2.0	7739	287	33.0	25.2	350.4	6.1
Kahului	20.89738	-156.46047	7/20/2013 9:26	2.0	16487	357	32.9	25.4	164.9	6.1
Kahului	20.89725	-156.45710	7/20/2013 9:31	1.6	7640	350	31.8	25.5	144.3	6.2
Kahului	20.89738	-156.45362	7/20/2013 9:36	2.2	4967	311	32.3	25.3	82.5	6.3
Kahului	20.89673	-156.45087	7/20/2013 9:41	1.4	7883	337	32.4	25.3	226.8	6.4
Kahului	20.89760	-156.44785	7/20/2013 9:46	1.3	4403	151	32.8	25.6	164.9	6.4
Kahului	20.89892	-156.44768	7/20/2013 9:51	1.7	2943	190	32.2	25.4	226.8	6.5
Kahului	20.89963	-156.44607	7/20/2013 9:56	1.7	2297	122	32.5	25.0	288.6	6.6
Kahului	20.89950	-156.44490	7/20/2013 10:01	0.9	5999	85	32.2	25.3	329.8	6.7
Kahului	20.90000	-156.44427	7/20/2013 10:06	1.1	3660	299	31.7	25.4	371.1	6.6
-	-	-	-	-	-		-	-	-	-
Honolua	21.01325	-156.63827	8/2/2012 13:09	0.4	153	26	34.9	26.6	101.0	5.6
Honolua	21.01397	-156.63787	8/2/2012 13:14	0.1	1535	108	34.9	26.6	201.9	5.5
Honolua	21.01515	-156.63826	8/2/2012 13:19	0.1	1831	151	34.7	26.1	60.9	5.4
Honolua	21.01642	-156.63948	8/2/2012 13:24	1.2	3057	209	34.3	26.0	201.9	5.4
Honolua	21.01687	-156.63999	8/2/2012 13:29	1.4	1791.5	79	34.7	26.7	101.2	5.2
Honolua	21.01740	-156.64005	8/2/2012 13:34	1.3	690	83	34.8	26.7	121.1	5.1
Honolua	21.01833	-156.64112	8/2/2012 13:39	0.8	2390	176	34.9	26.6	60.6	5
Honolua	21.01382	-156.64090	8/3/2012 14:54	2.0	7768	89	35.0	25.8	40.4	5.7
Honolua	21.01333	-156.63968	8/3/2012 14:59	2.0	1750	138	34.9	25.9	40.4	5.8
Honolua	21.01357	-156.63951	8/3/2012 15:04	3.0	652	50	34.9	25.8	80.8	5.4
Honolua	21.01337	-156.63900	8/3/2012 15:09	3.0	990	44	35.0	25.6	60.6	5.3

Field Area	Latitude	Longitude	Date/Time	Mixed layer depth (cm)	Surface Area (m^2)	Shoreline Length (m)	Salinity	Water Temp (°c)	Rn activity in air (Bq/m^3)	Wind Speed (m/s)
-	-	-	-	-	-		-	-	-	-
Waiehu	20.91737	-156.49048	7/21/2013 8:55	0.5	3006	53	31.4	25.5	0.0	6
Waiehu	20.91730	-156.49120	7/21/2013 9:00	0.4	4613	127	30.2	25.6	0.0	5.9
Waiehu	20.91655	-156.49157	7/21/2013 9:05	0.4	3002	114	29.9	25.6	103.1	5.8
Waiehu	20.91565	-156.49155	7/21/2013 9:10	0.5	1789	78	30.6	25.6	123.7	5.9
Waiehu	20.91512	-156.49138	7/21/2013 9:15	0.5	1607	64	30.9	25.6	144.3	6
Waiehu	20.91467	-156.49118	7/21/2013 9:20	0.8	2042	95	30.9	25.6	123.7	6.1
Waiehu	20.91390	-156.49087	7/21/2013 9:25	1.0	2215	106	31.5	25.6	41.2	6.1
Waiehu	20.91310	-156.49043	7/21/2013 9:30	0.9	4330	196	32.5	25.5	123.7	6.2
Waiehu	20.91170	-156.48952	7/21/2013 9:35	0.4	4282	225	33.7	25.6	20.6	6.3
Waiehu	20.91045	-156.48802	7/21/2013 9:40	0.4	8377	253	34.6	25.7	20.6	6.4
Waiehu	20.91051	-156.48636	7/21/2013 9:45	0.0	32895	298	34.8	25.8	103.1	6.4
-	-	-	-	-	-		-	-	-	-
Honomanu	20.86324	-156.16371	7/13/2013 14:32	1.0	4092	197	34.2	24.5	150.3	4.9
Honomanu	20.86150	-156.16454	7/13/2013 14:37	1.0	1847	197	31.0	24.1	601.0	4.9
Honomanu	20.86129	-156.16576	7/13/2013 14:42	2.0	734	213	28.7	23.9	279.5	4.9
Honomanu	20.86261	-156.16628	7/13/2013 14:47	2.0	1932	305	32.5	24.2	247.4	4.9
Honomanu	20.86443	-156.16628	7/13/2013 14:52	1.0	3706	188	33.7	24.3	184.8	4.9

A 5. Parameters for radon time series stations and radon surveys. The type of model the sample was applied to, either a time series (TS), survey, or both is shown.

Field area	Sample Name	Latitude	Longitude	Sample Date	Temp. (°C)	Sal	^{222}Rn in (dpm/L)	TS/Survey
Kuau	TVP3	20.92613	-156.3698	7/7/2013	21.8	0.9	239.1	Both
Maalaea	MP1_14	20.79213	-156.5097	3/30/2014	25.1	1.2	639.1	Both
Kahului	KWP3	20.89895	-156.4467	7/20/2013	26.6	7.5	153.3	Survey
Kahului	KWP1_14	20.89643	-156.4535	3/29/2014	24.7	19.0	217.3	TS
Honolua	HBP3_12	21.01250	-156.63763	8/2/2012	23.2	0.7	386.8	Survey
Honolua	HBSP3	21.01342	-156.64070	4/1/2014	20.2	3.5	106.3	TS
Waiehu	WBP1	20.91534	-156.49173	7/21/2013	26.7	24.9	176.5	Survey
Waiehu	WP2_14	20.91708	-156.49190	3/28/2014	24.0	1.7	114.2	TS
Honomanu	HMS-2	20.86058	-156.16521	7/12/2013	19.3	0.4	170.1	Survey
Honomanu	HMP-1	20.86052	-156.16563	4/3/2014	22.3	8.2	155.2	TS